ACS OMEGA

http://pubs.acs.org/journal/acsodf

Article

# New Benzimidazole-, 1,2,4-Triazole-, and 1,3,5-Triazine-Based Derivatives as Potential EGFR$^{WT}$ and EGFR$^{T790M}$ Inhibitors: Microwave-Assisted Synthesis, Anticancer Evaluation, and Molecular Docking Study

Heba E. Hashem, Abd El-Galil E. Amr,* Eman S. Nossier, Manal M. Anwar,* and Eman M. Azmy

Cite This: *ACS Omega* 2022, 7, 7155−7171

Read Online

ACCESS | Metrics & More | Article Recommendations | Supporting Information

**ABSTRACT:** A new series of benzimidazole, 1,2,4-triazole, and 1,3,5-triazine derivatives were designed and synthesized using a microwave irradiation synthetic approach utilizing 2-phenylacetyl isothiocyanate (**1**) as a key starting material. All the new analogues were evaluated as anticancer agents against a panel of cancer cell lines utilizing doxorubicin as a standard drug. Most of the tested derivatives exhibited selective cytotoxic activity against MCF-7 and A-549 cancer cell lines. Furthermore, the new target compounds **5**, **6**, and **7** as the most potent antiproliferative agents have been assessed as *in vitro* EGFR$^{WT}$ and EGFR$^{T790M}$ inhibitors compared to the reference drugs erlotinib and AZD9291. They represented more potent suppression activity against the mutated EGFR$^{T790M}$ than the wild-type EGFR$^{WT}$. Moreover, the compounds **5**, **6**, and **7** down-regulated the oncogenic parameter p53 ubiquitination. A docking simulation of compound **6b** was carried out to correlate its molecular structure with its significant EGFR inhibition potency and its possible binding interactions within the active site of EGFR$^{WT}$ and the mutant EGFR$^{T790M}$.

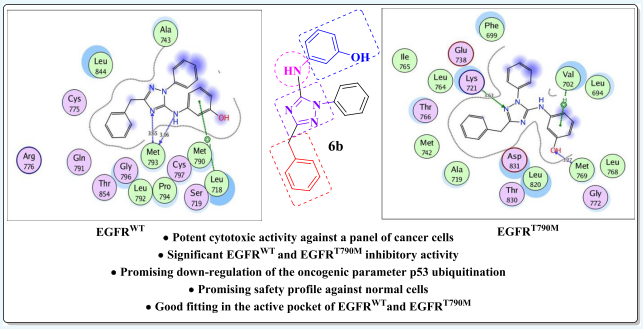


## 1. INTRODUCTION

Cancer disease is a terrible health epidemic that kills millions of people all over the world in both developed and developing countries.[1] Despite the great progress accomplished in cancer therapy, several limitations still present. Examples are the selectivity for cancer cells, adverse effects, as well as the multiple-drug resistance acquisition by the cancer cells leading them to be unresponsive to conventional therapeutic agents.[2,3] Accordingly, the innovation of new small molecules that are both potent and selective is still a serious challenge in the field of medicinal chemistry. The alteration of different protein expressions and the activity of various receptor tyrosine kinases (RTKs) are considered the main causes of many cancer types since they are responsible for the regulation of different cellular pathways such as proliferation, differentiation, migration, and angiogenesis.[4,5] The epidermal growth factor receptor (EGFR) is a member of tyrosine kinases (TKs).[6] It is a trans-membrane protein belonging to the erbB/HER-family and plays a pivotal role in governing cellular transduction or communication signaling through the phosphorylation of tyrosine residues in the protein domain.[7,8] EGFR is one of the main tumor markers in many cancer types (such as colon, lung, liver, cervical, ovarian, breast, prostate, and bladder cancers), where its signaling in tumors, as opposed to normal cells, becomes dysregulated, resulting in EGFR overexpression and/or obtaining a gain-of-function mutation.[9−13] This act is considered the main cause of tumor cell proliferation, invading the surrounding tissues and resulting in an increased angiogenesis.[14] Accordingly, interrupting EGFR communicating signals is considered to be one of the prime targets to invade tumors caused by its mis-regulation.[9−14] Targeted drugs inhibiting EGFR can selectively attack the cancer cells rather than normal ones, thus producing a good safety profile and less harm to the body with more patient comfortability.[15] Multiple EGFR suppressors have been developed and classified into different generations. The first generation was gefitinib (Iressa), erlotinib (Tarceva), and icotinib (Conmana).[16−20] Studies revealed that acquired drug resistance to the first-generation EGFR-TKIs was revealed due to T790M "gatekeeper" and L858R mutations in EGFR about 9−14 months after clinical treatment.[21−23] The emergence of resistance paved the way toward the development of the second-generation inhibitors (EGFR TKI) (afatinib, dacomitinib,

**Received:** December 3, 2021
**Accepted:** January 24, 2022
**Published:** February 18, 2022

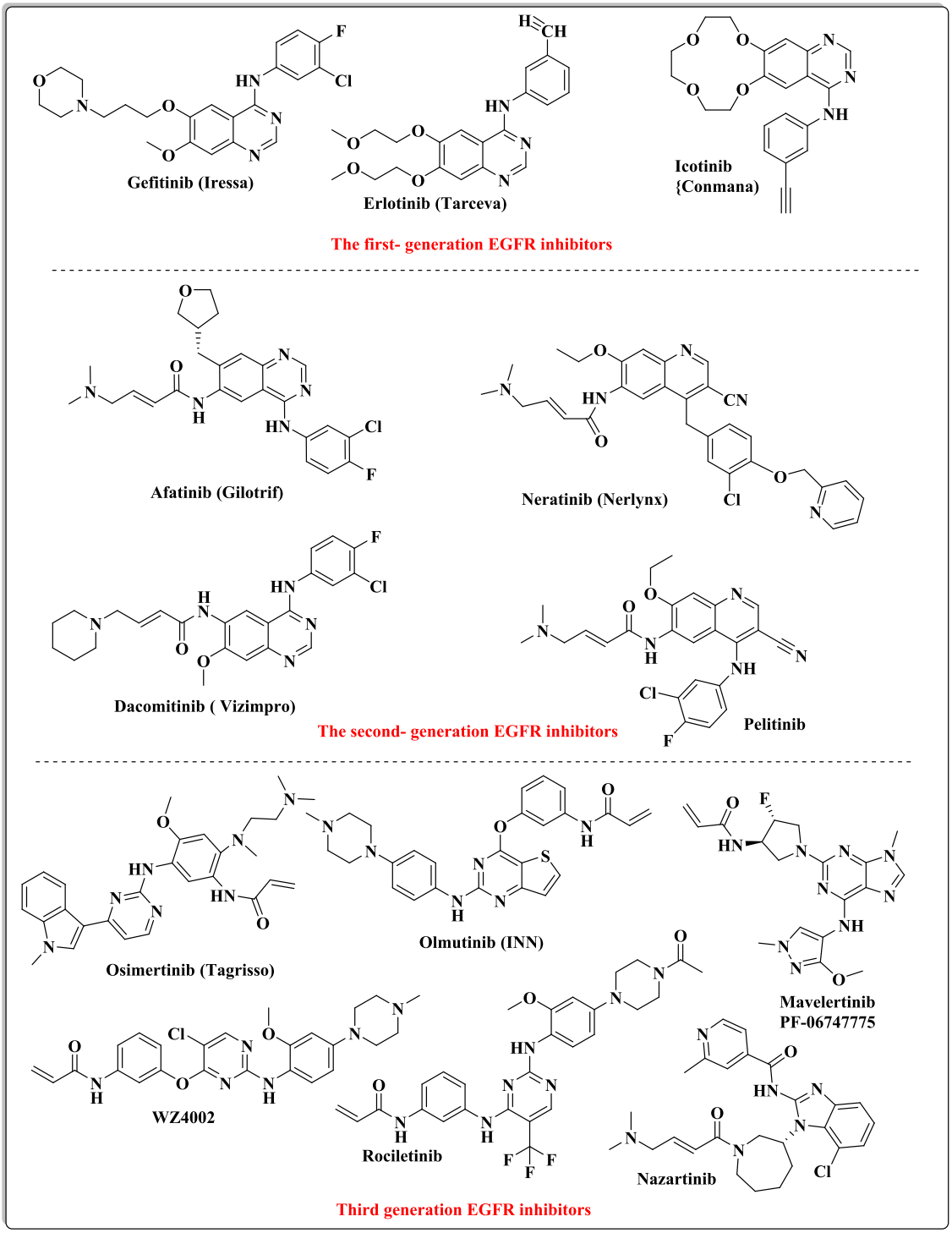


**Figure 1.** Examples of the first, second and third generations of EGFR inhibitors.

neratinib, and canertinib) that have exhibited a 60−70% objective response rate.[17] The drugs related to this class contain an electrophilic acrylamide side chain that interacts irreversibly with cysteine CYS797 forming covalent complexes, thus overcoming the obstacle of resistance mediated by $EGFR^{T790M}$ or $EGFR^{T790M/L858R}$ mutation.[24−27] On the other hand, due to the high reactivity of the acrylamide moiety, it interacts non-selectively with the cysteine residue in untargeted proteins, leading to toxic side effects such as diarrhea and skin rash that limited their clinical use.[28−32] Recently, to solve these undesirable side effects, several third-generation inhibitors have been discovered, such as WZ4002,[29] osimertinib (AZD9291) (Tagrisso),[33] olmutinib (Olita),[31] and rociletinib (CO1686).[34] These inhibitors do not only produce good anti-tumor activity but also produce good selectivity to $EGFR^{T790M}$ and $EGFR^{T790M/L858R}$ kinases.[29,35] Rociletinib and osimertinib were considered as breakthrough therapies in the mutant NSCLC treatment by the US FDA in 2014.[36] Studies showed that osimertinib's efficacy is marred by various side effects such as grade 3 venous thromboembolism and pneumonia. Its toxicity was attributed to AZ5104, which is its main metabolite, lacking selectivity between the mutant and WT EGFR.[29,35−38]



https://doi.org/10.1021/acsomega.1c06836
ACS Omega 2022, 7, 7155−7171

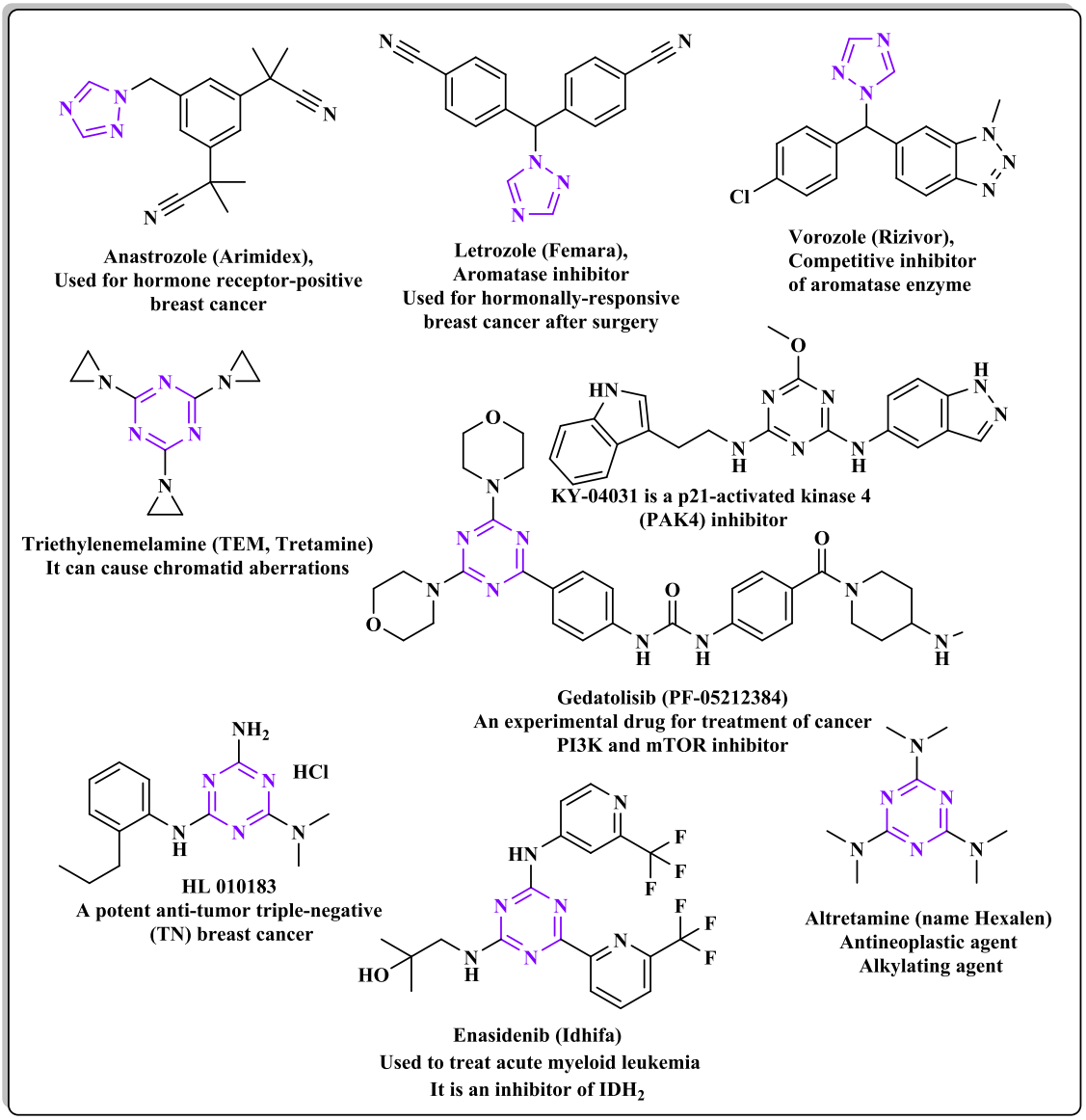


**Figure 2.** Examples of various marketed anticancer drugs bearing 1,2,4-triazole and *s*-triazine scaffolds.

Accordingly, much efforts are still needed to discover new EGFR inhibitors of high selectivity to $EGFR^{T790M}$ and $EGFR^{T790M/L858R}$ kinase with low side effects (Figure 1).

Many nitrogen-heterocyclic ring systems have recently been discovered to introduce surprisingly complex biological properties, making them one of the most significant groups in medicinal chemistry. They constitute a basic scaffold in numerous drugs due to their capabilities to imitate and interact with different biological molecules, leading to remarkable pharmacological properties.[39−42] The benzimidazole scaffold participates in various compounds producing a wide range of biological activities such as antimicrobial, antiparasitic, antihistaminic, antiallergic, anticancer, and antioxidant.[43−49] The benzimidazoles could be considered as auxiliary isosters of nucleotides having a potential for chemotherapeutic applications.[46] In addition, the orally available third-generation EGFR inhibitor nazartinib bears a benzimidazole nucleus.[50] Moreover, the triazole nucleus plays a vital role in the field of drug discovery. The triazole ring is characterized by significant stability and excellent pharmacological potency due to its electron-rich characteristics and the occurrence of an unsaturated hydrocarbon ring structure. These properties support the triazole structure to interact with various receptors (enzymes) through H-bonding that endows it with significant pharmacological actions.[51−53] Currently, triazole derivatives are used to treat a wide variety of diseases specially cancer disease.[51−53] Numerous anticancer drugs bearing the 1,2,4-triazole moiety are available in the market such as anastrozole,[54,55] letrozole,[56] and vorozole.[57] Furthermore, the *s*-triazine (1,3,5-triazine) scaffold constitutes a basic template for the design and synthesis of various bioactive compounds with widespread applications in medicinal chemistry.[58] The *s*-triazine core has three functionalized branches at positions 2, 4, and 6, a property that leads to easily modulating the physicochemical and biological activities of *s*-triazine derivatives.[59] Many studies investigated the notable progress in the design, synthetic approaches, and evaluation of numerous *s*-triazine candidates with great promising antitumor activity acting via the inhibition of different protein kinases such as CDK2, PI3K$\alpha$/mTOR, CA, human topoisomerase II$\alpha$, hDHFR, EGFR ($EGFR^{WT}$ and $EGFRT^{790M}$), and tubulin polymerization.[60−67] There are various anticancer drugs



https://doi.org/10.1021/acsomega.1c06836
ACS Omega 2022, 7, 7155−7171

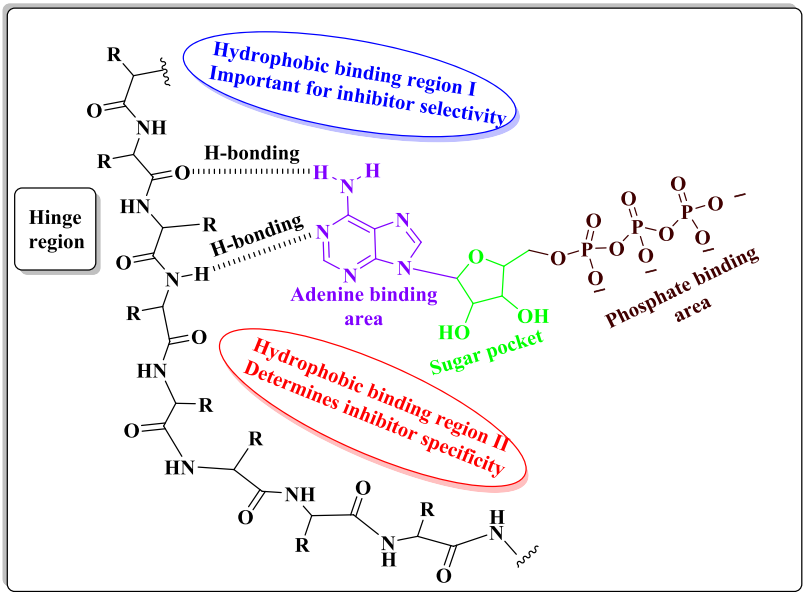


**Figure 3.** The structure of the ATP-binding site of EGFR-TK.

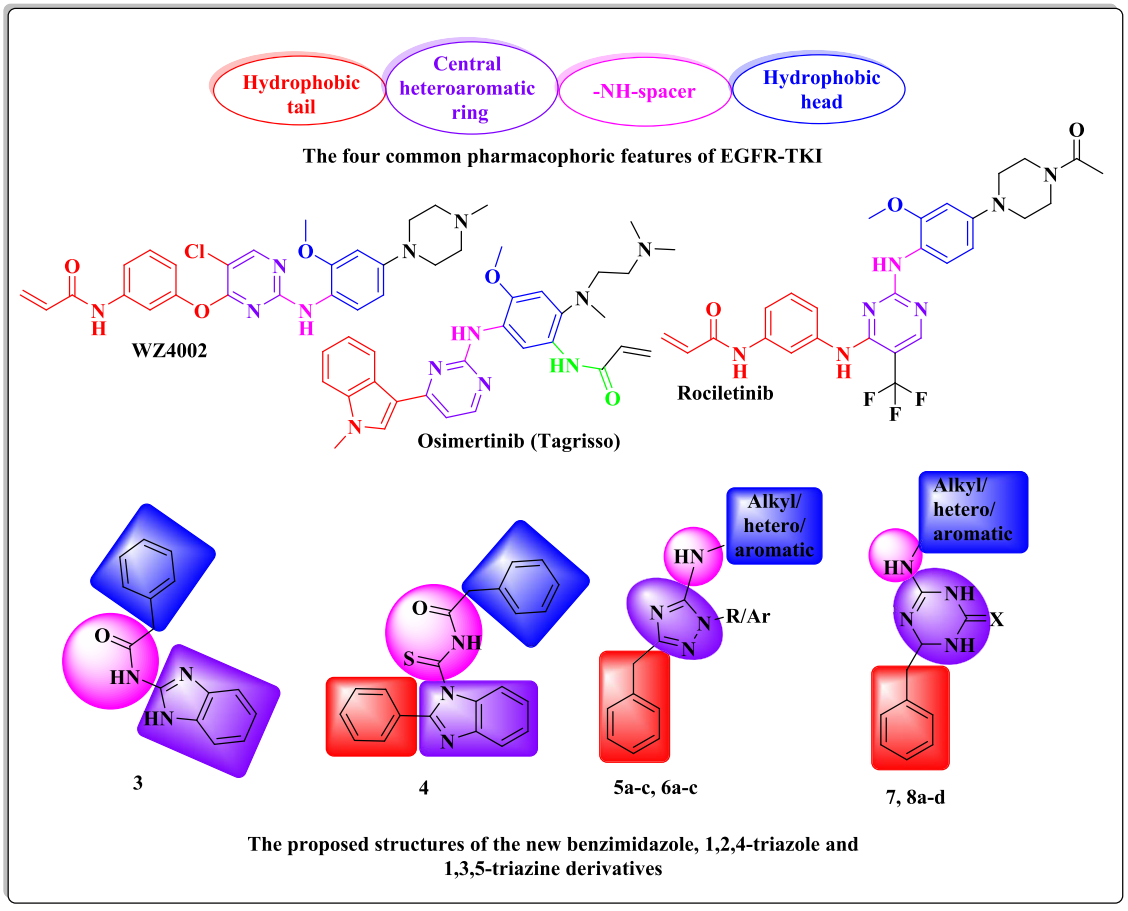


**Figure 4.** The designed molecular structures of new benzimidazole, 1,2,4-triazole, and 1,3,5-triazine derivatives.

containing the *s*-triazine motif that are FDA-approved such as tretamine,[68] gedatolisib,[69] HL 010183,[70] enasidenib,[71] altretamine,[72] and KY-04031[73] (Figure 2).

Microwave-assisted organic synthesis (MAOS) has been widely used in green chemistry in recent years.[74] Microwave irradiation is an eco-friendly approach without hazardous solvents. It helps in the synthesis of various heterocyclic compounds rapidly and in high yields.[75,76] In addition, MAOS has a great contribution in chemical selectivity, catalyst-free conditions, and the absence of side products during the synthesis processes of various aromatic and heterocyclic compounds.[77,78] Based on the above-mentioned knowledge



https://doi.org/10.1021/acsomega.1c06836
ACS Omega 2022, 7, 7155−7171

**Scheme 1. Synthesis of New Substituted Benzimidazole Derivatives Utilizing the Microwave Irradiation Synthetic Approach**

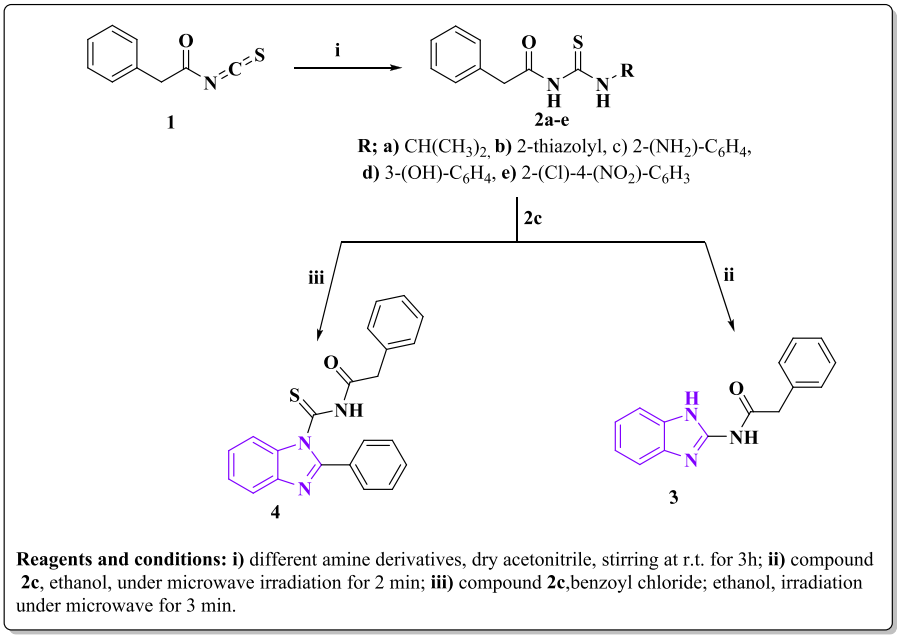


**Scheme 2. Synthesis of New Substituted 1,2,4-Triazole and 1,3,5-Triazine Derivatives Utilizing the Microwave Irradiation Synthetic Approach**

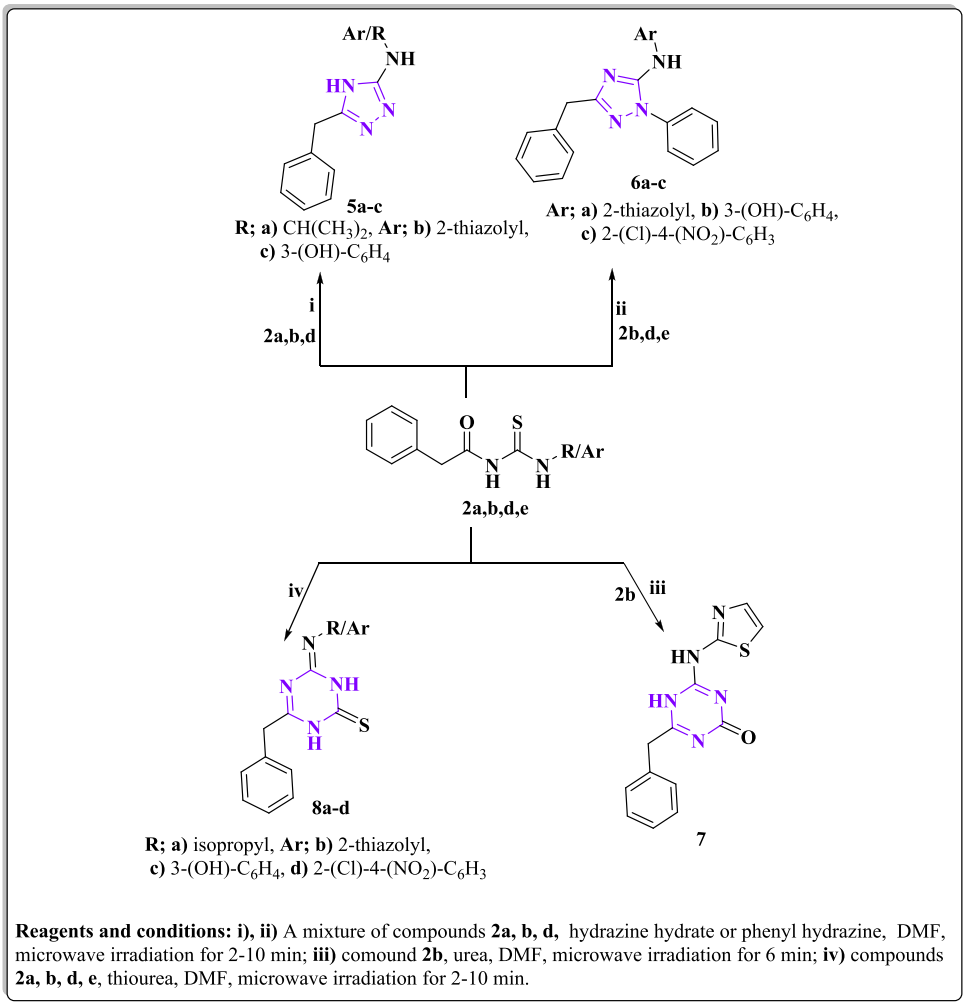




https://doi.org/10.1021/acsomega.1c06836
ACS Omega 2022, 7, 7155−7171

and in continuation of our previous efforts in the field of design and generation of new bioactive heterocyclic compounds,[79−84] this study deals with the design and microwave-assisted organic synthesis of a new set of benzimidazole, 1,2,4-triazole, and *s*-triazine derivatives targeting the wild-type EGFR-TK ($EGFR^{WT}$) and the mutant EGFR-TK ($EGFRT^{790M}$).

**1.1. Rational and Design.** Computational studies represented that the ATP active pocket of EGFR-TK possesses mainly five regions, as follows: (1) an adenine binding pocket bearing the key amino acid residues that can interact with the adenine ring via hydrogen bond formation, (2) a sugar zone (hydrophilic ribose pocket), (3) hydrophobic zone I (this area is not used by ATP but displays a pivotal role in the inhibitor selectivity), (4) hydrophobic region II (this area is also not used by ATP and can be used to determine the inhibitor specificity), and (5) a phosphate binding area that is important for improving the characteristics of inhibitor pharmacokinetics[85,86] (Figure 3).

Additionally, various studies demonstrated that the main pharmacophoric features shared by multiple EGFR-TKIs are four common areas: (i) a flat hetero-aromatic ring system, fitting in the adenine binding pocket and that can participate in H-bonding interactions with different amino acids such as Met793, Thr854, and Thr790 residues; (ii) a terminal hydrophobic head that occupies the hydrophobic zone I; (iii) an imino moiety (NH− spacer) that can participate in generating hydrogen bonds with different amino acid residues present in the linker region; and (iv) a hydrophobic tail that fits in the hydrophobic region II[87−89] (Figure 4).

Since benzimidazole, 1,2,4-triazole, and *s*-triazine are bioisosteric, this work deals with the design and MAOS synthesis of new sets bearing one of the previously mentioned heterocyclic nuclei possessing the essential pharmacophoric features of EGFR-TKIs. The first position was the benzimidazole moiety (as compounds **3** and **4**), and this scaffold was replaced by 1,2,4-triazole (as compounds **5** and **6**) and 1,3,5-triazine nuclei (as compounds **7** and **8**) to fit in the adenine binding pocket, where the heterocyclic nitrogen atoms act as hydrogen-bond acceptors leading to excellent EGFR-TK potency.[90] The second position was the terminal benzyl moiety (hydrophobic head) (as compounds **3** and **4**), which might be replaced with aliphatic, heterocyclic, or substituted phenyl structures (as compounds **5**−**8**). The third position was the NH linker, as a site for the creation of different hydrogen bonds. The used linkers may be an imino group as in compounds **5**−**8** or a carbonothioyl-acetamide linker (as in compound **4**). The fourth position was the phenyl group (hydrophobic tail), where a phenyl ring was incorporated at position-2 of the benzimidazole nucleus as in compound **4** or replaced by a benzyl ring at positions-5/3 of the 1,2,4-triazole nucleus or position-6 of the triazine ring to occupy the hydrophobic zone II of the ATP binding site. The fourth position of the benzimidazole **3** was left unsubstituted to find out the impact of the phenyl substitution on the target activity (Figure 4).

All the newly synthesized compounds were screened for their anti-proliferative activities against a panel of human cancer cell lines. Furthermore, the most promising compounds as cytotoxic agents were assessed as $EGFR^{WT}$, $EGFR^{T790M}$, and p53 ubiquitination inhibitors. Since compound **6b** represented the most promising cytotoxic activity as well as $EGFR^{WT}$ and $EGFR^{T790M}$ inhibition activity, it was selected as a representative example to emphasize its possible binding patterns in the active pockets of $EGFR^{WT}$ and $EGFR^{T790M}$ via a molecular docking study.

## 2. RESULTS AND DISCUSSION

**2.1. Chemistry.** The new target compounds **3**−**8** were synthesized in short reaction times and with high yields utilizing a microwave irradiation process (Schemes 1 and 2, Table 1). The chemical structures of the new compounds were

**Table 1. The Reaction Times and the Yields of the Newly Synthesized Compounds Using the Microwave Irradiation Technique**

| | microwave irradiation method | |
|---|---|---|
| compound no. | time (min) | yield (%) |
| **3** | 2 | 80 |
| **4** | 3 | 96 |
| **5a** | 2 | 98 |
| **5b** | 5 | 96 |
| **5c** | 7 | 86 |
| **6a** | 6 | 95 |
| **6b** | 9 | 85 |
| **6c** | 10 | 89 |
| **7** | 5 | 97 |
| **8a** | 4 | 96 |
| **8b** | 9 | 97 |
| **8c** | 7 | 92 |
| **8d** | 10 | 98 |

elucidated using microanalytical and spectral data (IR, $^1H$, $^{13}C$ NMR, MS). 2-Phenylacetyl isothiocyanate (**1**) was utilized as a key starting material and treated with different aliphatic, heterocyclic, and/or aromatic amines, namely, isopropylamine, 2-aminothiazole, *o*-phenylenediamine, *m*-aminophenol, and *o*-chloro-*p*-nitroaniline, in acetonitrile at room temperature[91] to afford the corresponding thiourea derivatives **2a**−**e**, respectively. IR spectra of **2a**−**e** represented characteristic absorption bands at the regions 3370−3135, 1690−1660, and 1173−1146 $cm^{-1}$ due to NH, C═O, and C═S groups, respectively. $^1H$ NMR spectra of the new compounds **2a**−**e** revealed singlet signals at the range $\delta$ 3.43−3.82 ppm representing the two methylene protons of $C\underline{H}_2$-ph. In addition, the expected signals of the aromatic protons appeared at the corresponding region $\delta$ 7.20−8.61 ppm, while the two NH protons appeared as $D_2O$ exchangeable signals at the range $\delta$ 12.11−13.0 ppm. Compound **2a** exhibited a doublet signal at $\delta$ 1.06 ppm and another multiplet at $\delta$ 3.80−3.84 ppm that is an evidence of the presence of the $-CH(CH_3)_2$ group. Compounds **2c** and **2d** exhibited two additional $D_2O$ exchangeable signals at $\delta$ 5.01 and 9.66 ppm due to $NH_2$ and OH groups, respectively.

Microwave irradiation of the thiourea derivative **2c** in DMF for 2 min led to its cyclization, forming the corresponding *N*-(1*H*-benzo[*d*]imidazol-2-yl)-2-phenylacetamide benzimidazole (**3**), while its microwave irradiation with benzoyl chloride afforded[92,93] the corresponding *N*-(2-phenyl-1*H*-benzo[*d*]-imidazole-1-carbonothioyl) benzamide (**4**) (Scheme 1). IR spectra of the later derivatives **3** and **4** exhibited absorption bands at the ranges 3220−3128 and 1670−1699 $cm^{-1}$ correlated to NH and C═O groups, respectively. Furthermore, **4** represented an additional band at 1266 $cm^{-1}$ due to its C═S moiety. $^1H$ NMR spectra of compounds **3** and **4** exhibited singlet signals at the region $\delta$ 3.70−3.91 due to $C\underline{H}_2$-ph and $D_2O$ exchangeable signals at the range $\delta$ 11.74−12.78



https://doi.org/10.1021/acsomega.1c06836
ACS Omega 2022, 7, 7155−7171

Table 2. *In Vitro* Cytotoxic Potency of the Newly Synthesized Compounds 2−8 against Various Human Cancer Cell Lines and Normal Cells Representing SI of the Most Active Derivatives[a]

| compd. no. | $IC_{50}$ (mean ± SEM) (μM) | | | | |
|---|---|---|---|---|---|
| | HepG-2 | PC-3 | MCF-7 | A-549 | PBMC |
| **2a** | 57.85 ± 0.07 | 26.82 ± 2.21 | 37.73 ± 0.08 | 34.57 ± 0.06 | 121.34 ± 11.35 |
| **2b** | 60.85 ± 0.06 | 44.50 ± 3.51 | 55.44 ± 0.04 | 57.48 ± 0.05 | 133.30 ± 13.67 |
| **2c** | 47.66 ± 0.04 | 25.44 ± 0.04 | 21.76 ± 0.08 | 27.81 ± 0.04 | 144.56 ± 14.89 |
| **2d** | 34.77 ± 0.03 | 39.32 ± 0.0 | 24.74 ± 0.08 | 20.84 ± 0.04 | 157.78 ± 16.35 |
| **2e** | 37.76 ± 0.05 | 40.56 ± 0.05 | 25.64 ± 0.08 | 25.96 ± 0.05 | 168.54 ± 17.36 |
| **3** | 37.73 ± 0.02 | 17.29 ± 0.03 | 6.59 ± 0.07 | 10.42 ± 0.05 | 179.25 ± 18.75 |
| **4** | 56.65 ± 0.04 | 25.41 ± 0.05 | 8.32 ± 0.04 | 15.61 ± 0.06 | 186.68 ± 19.36 |
| **5a** | 35.66 ± 0.04 | 16.49 ± 0.05 | 5.42 ± 0.05 | 10.37 ± 0.04 | 174.90 ± 18.24 |
| | SI = 4.90 | SI = 10.60 | SI = 32.26 | SI = 16.86 | |
| **5b** | 38.49 ± 0.02 | 18.22 ± 0.03 | 4.18 ± 0.03 | 8.27 ± 0.03 | 165.76 ± 17.36 |
| | SI = 4.30 | SI = 9.09 | SI = 39.65 | SI = 20.04 | |
| **5c** | 27.59 ± 0.04 | 18.44 ± 0.04 | 4.33 ± 0.04 | 12.30 ± 0.04 | 146.32 ± 16.15 |
| | SI = 5.23 | SI = 7.93 | SI = 33.79 | SI = 11.89 | |
| **6a** | 10.48 ± 0.03 | 16.30 ± 0.09 | 4.30 ± 0.04 | 5.20 ± 0.03 | 157.45 ± 16.89 |
| | SI = 15.02 | SI = 9.65 | SI = 36.61 | SI = 30.27 | |
| **6b** | 5.47 ± 0.02 | 13.21 ± 0.06 | 1.29 ± 0.03 | 3.18 ± 0.03 | 178.23 ± 17.69 |
| | SI = 32.58 | SI = 13.49 | SI = 138.16 | SI = 56.04 | |
| **6c** | 7.73 ± 0.04 | 26.41 ± 0.05 | 2.51 ± 0.06 | 5.80 ± 0.05 | 187.67 ± 19.76 |
| | SI = 24.27 | SI = 7.10 | SI = 74.76 | SI = 32.35 | |
| **7** | 29.75 ± 0.03 | 17.90 ± 0.03 | 4.65 ± 0.07 | 7.43 ± 0.04 | 165.23 ± 18.05 |
| **8a** | 59.84 ± 0.05 | 36.55 ± 0.03 | 13.75 ± 0.08 | 25.46 ± 0.05 | 173.45 ± 18.95 |
| | SI = 2.91 | SI = 4.74 | SI = 12.61 | SI = 6.81 | |
| **8b** | 60.48 ± 0.05 | 42.56 ± 0.06 | 17.95 ± 0.04 | 37.21 ± 0.03 | 196.67 ± 20.67 |
| | SI = 3.25 | SI = 4.62 | SI = 10.95 | SI = 5.28 | |
| **8c** | 45.49 ± 0.04 | 32.48 ± 0.04 | 10.31 ± 0.04 | 8.29 ± 0.03 | 188.89 ± 19.86 |
| | SI = 4.15 | SI = 5.81 | SI = 18.32 | SI = 22.78 | |
| **8d** | 47.86 ± 0.05 | 39.55 ± 0.08 | 14.77 ± 0.05 | 9.50 ± 0.06 | 179.09 ± 18.96 |
| | SI = 3.74 | SI = 4.52 | SI = 12.12 | SI = 18.85 | |
| DOX | 4.51 ± 0.26 | 8.11 ± 0.05 | 4.17 ± 0.2 | 8.20 ± 0.08 | 250.00 ± 26.56 |
| | SI = 55.43 | SI = 30.82 | SI = 59.95 | SI = 30.48 | |
| erlotinib | 8.19 ± 0.4 | 8.89 ± 0.6 | 4.16 ± 0.2 | 3.76 ± 0.2 | 45.75 ± 26.56 |
| | SI = 5.58 | SI = 5.14 | SI = 10.99 | SI = 12.16 | |

[a]DOX: doxorubicin; $IC_{50}$: compound concentration required to inhibit the cell viability by 50%; SEM: standard error mean; each value is the mean of three independent determinations; SI: selectivity index.

ppm representing NH groups, while the aromatic-Hs appeared as multiplet signals at their expected up-field region δ 7.36−8.24 ppm. Moreover, $^{13}$C NMR spectra of both **3** and **4** showed signals at the corresponding regions δ 40.06 and 40.32 ppm referring to $\underline{C}H_2$-ph and δ 173.30 and 167.0 due to C═O groups as well as various signals at the range δ 114.05−166.53 ppm representing the aromatic carbons.

On the other hand, treatment of compounds **2a**, **b**, **d**, and **e** with hydrazine hydrate or phenyl hydrazine under microwave irradiation afforded the corresponding 1,3,4-triazole derivatives **5a−c** and **6a−c**, respectively, as the reported methods.[91−94] IR spectral data of the latter triazole derivatives were devoid of any absorption bands correlated to C═O or C═S groups; instead, they exhibited absorption bands at 3288−3199 $cm^{-1}$ contributing to NH groups, 3328 $cm^{-1}$ referring to OH of compound **5c**, and 1664−1639 $cm^{-1}$ due to C═N groups. Furthermore, $^1$H NMR data of compounds **5** and **6** showed singlet signals at the region δ 4.23−3.50 ppm representing the presence of the two methylene protons of $CH_2$-ph and $D_2O$ exchangeable signals at the range δ 7.21−12.31 ppm due to NH and OH protons, in addition to the expected multiplet signals at δ 6.60−8.38 ppm representing the aromatic protons. The $-CH(CH_3)_2$ residue of **5a** was confirmed by the presence of doublet−multiplet signals at δ 1.06 and 3.39 ppm. $^{13}$C NMR spectra of compounds **5** and **6** represented singlet signals at the range δ 38.83−42.07 ppm ascribed to $\underline{C}H_2$-ph and different signals at the region δ 102.52−170.51 ppm referring to the aromatic carbons. Also, the isopropyl residue of **5a** appeared as two additional singlets at δ 22.86 and 39.84 ppm.

Furthermore, cyclization of the thiazolyl derivative **2b** with urea using microwave irradiation gave the corresponding 1,3,5-triazin-2-one derivative **7**. On the other hand, microwave irradiation of compounds **2a**, **b**, **d**, and **e** with thiourea led to the formation of the corresponding 1,3,5-triazin-2-thione analogues **8a−d**, respectively (Scheme 2), following the reported reactions.[91−94] The IR spectrum of compound **7** showed a characteristic absorption band at 1685 $cm^{-1}$ characteristic for the carbonyl group of the triazine ring, in addition to an absorption band at 3206 $cm^{-1}$ due to NH moieties. IR spectra of compound **8** exhibited the C═S group as an absorption band at the region1177−1127 $cm^{-1}$. Moreover, $^1$H NMR data of compound **8** exhibited $C\underline{H}_2$-ph protons as a singlet signal at δ 3.51−3.82 ppm, the aromatic protons as multiplet signals in the down field expected region δ 6.65−7.76 ppm, and NH and OH protons as $D_2O$ exchangeable singlets at the region δ 7.96−12.35 ppm. The isopropyl protons of compound **8a** appeared as a doublet−multiplet signal at δ 1.05 and 3.36 ppm. In addition, $^{13}$C NMR spectra showed signals at δ 40.06−42.15 ppm due to $CH_2$-ph, 22.85 and 40.15 due to $-CH(CH_3)_2$ of compound **8a**, and 113.65−170.75 related to the aromatic carbons. Further support for the suggested structures of the new compounds



https://doi.org/10.1021/acsomega.1c06836
ACS Omega 2022, 7, 7155−7171

was gained by their mass spectra, which were in accordance with the proposed structures representing their correct molecular ion peaks beside some other important peaks (cf. Experimental Section).

**2.2. Biological Activity.** *2.2.1. In Vitro Evaluation of Cytotoxic Potentials of the Newly Prepared Derivatives.* The newly synthesized compounds **2**−**8** were investigated for their potential cytotoxic activities against a panel of four different human cancer cell lines—hepatocellular carcinoma (HepG-2), prostate carcinoma (PC-3), breast adenocarcinoma (MCF-7), and non-small cell lung cancer cells (A-549)—and the normal peripheral blood mononuclear cells (PBMCs) using an MTT assay.[95] Doxorubicin and erlotinib served as reference standards. The concentrations of the tested derivatives that induced 50% inhibition of the cell viability ($IC_{50}$, $\mu$M) were determined and tabulated in Table 2.

Based on the resultant data, the examined compounds showed versatile antiproliferative activities against the tested cell lines. It could be noted that the benzimidazole derivatives **3** and **4**, the triazole derivatives **5** and **6**, and the triazine derivatives **7** and **8** elicited superior cytotoxicity against MCF-7 and A-549 cell lines. The *N*-phenyl-1,2,4-triazole compounds **6a**−**c** exhibited the most potent cytotoxic activity against MCF-7 of $IC_{50}$ values ranging from 1.29 to 4.30 $\mu$M that were evidently near those of the reference drugs (doxorubicin and erlotinib) of $IC_{50}$ 4.17 and 4.16 $\mu$M, respectively. Furthermore, the latter derivatives reduced the viability of A-549 cells with 1.3−2.6-folds more potency than doxorubicin and approximately equivalent potency to erlotinib, exhibiting $IC_{50}$'s ranging from 3.18 to 5.80 $\mu$M and $IC_{50doxorubicin,\ erlotinib}$ of 8.20 and 3.76 $\mu$M, respectively. The 3-OH-phenyl derivative **6b** was 3.2-folds more potent than doxorubicin and erlotinib against MCF-7 cells and 2.6-folds more potent than doxorubicin against the A-549 cell line. The oxygen atom of the hydroxyl group might produce an additional H-binding interaction with the target protein. In addition, the HepG-2 cell line exhibited promising sensitivity against **6a**−**c** that was slightly higher than its sensitivity against erlotinib but slightly less than that against doxorubicin, exhibiting $IC_{50}$'s of 5.47−10.48 $\mu$M and $IC_{50doxorubicin,\ erlotinib}$ of 4.51 and 8.19 $\mu$M.

Both MCF-7 and A-549 cell lines displayed an equipotent or a slightly less sensitivity against the 1,2,4-triazole analogues **5a**−**c** than that against the reference drugs, displaying $IC_{50}$'s ranging from 4.18 to 5.42 and 7.43 to 12.30 $\mu$M, respectively. Moreover, the 1,3,5-triazinone **7** was nearly equivalent to doxorubicin against MCF-7 and A-549 cell lines with $IC_{50}$'s of 4.65 and 7.43 $\mu$M, but it showed nearly 2-folds less potency against A-549 compared to erlotinib.

With the exception of compounds **8c** and **8d** that were as potent as doxorubicin against the A-549 cell line, a detectable drop in the cytotoxic activity was observed by the 1,3,5-triazin-2-thione derivatives **8** against both MCF-7 and A-549 cell lines with $IC_{50}$ values of 10.31−25.46 and 37.21−25.46 $\mu$M, respectively. On the other hand, the tested compounds showed moderate to weak antiproliferative activities against hepatocellular carcinoma (HepG-2) and prostate carcinoma (PC-3) cell lines. On the other hand, all the tested derivatives produced low cytotoxicity against the normal PBMC cell line with $IC_{50}$ values <100 $\mu$M, confirming the safety margin of the newly synthesized derivatives.

*2.2.2. In Vitro Inhibition of $EGFR^{WT}$ and $EGFR^{T790M}$ Activity.* Following the primary screening for cytotoxic potentials, the most active congeners **5a**−**c**, **6a**−**c**, and **7** that revealed the most promising antiproliferative activities were further investigated for their possible mechanism of actions against cancer cells. They were assessed in terms of *in vitro* kinase inhibitory efficiencies against the wild-type $EGFR^{WT}$ and the mutant form $EGFR^{T790M}$ using a homogeneous time resolved fluorescence (HTRF) assay.[96,97] The results are summarized as $IC_{50}$ values ($\mu$M) in Table 3 using erlotinib and AZD9291 as positive controls.

**Table 3. Kinase Inhibitory Assay of the Newly Synthesized Derivatives 5−7 in Comparison with Erlotinib and AZD9291 against $EGFR^{WT}$ and Mutant $EGFR^{T790M}$[a]**

| | $IC_{50}$ (mean ± SEM) ($\mu$M) | |
|---|---|---|
| compound no. | $EGFR^{WT}$ | $EGFR^{T790M}$ |
| erlotinib | 0.09 ± 0.05 | 0.55 ± 0.10 |
| AZD9291 | 0.52 ± 0.03 | 0.03 ± 0.01 |
| **5a** | 0.25 ± 0.01 | 0.17 ± 0.05 |
| **5b** | 0.22 ± 0.15 | 0.13 ± 0.11 |
| **5c** | 0.24 ± 0.30 | 0.14 ± 0.50 |
| **6a** | 0.18 ± 0.10 | 0.12 ± 0.18 |
| **6b** | 0.08 ± 0.05 | 0.09 ± 0.01 |
| **6c** | 0.15 ± 0.02 | 0.13 ± 0.07 |
| **7** | 0.22 ± 0.05 | 0.18 ± 0.11 |

[a]$IC_{50}$: compound concentration required to inhibit the enzymes' activities by 50%; SEM: standard error mean; each value is the mean of three independent values.

Excellent inhibitory activities were obtained by the examined compounds **5** and **6** against $EGFR^{WT}$, which were about 2−6.5 times more potent than AZD9291 representing $IC_{50}$ values ranging from 0.08 to 0.25 $\mu$M and $IC_{50AZD9291}$ of 0.52 $\mu$M. On the other hand, erlotinib ($IC_{50}$ of 0.095 $\mu$M) represented about 2.7−1.6-folds more potency against the wild form of EGFR compared with **5a**−**c** and **6a** and **c**. Interestingly, compound **6b** appeared to be a 1-fold more potent $EGFR^{WT}$ inhibitor than erlotinib with an $IC_{50}$ value of 0.08 $\mu$M. Additionally, the resultant data investigated that compounds **5a**−**c**, **6a**−**c**, and **7** were 6.1−3.2-folds more active against the mutated form of $EGFR^{T790M}$ than the reference drug erlotinib, exhibiting $IC_{50}$'s ranging from 0.09 to 0.18 $\mu$M and $IC_{50\ erlotinib}$ of 0.55 $\mu$M. Reversely, the tested analogues **5**, **6**, and **7** appeared to be less potent $EGFR^{T790M}$ suppressors compared to the reference drug AZD9291 with $IC_{50}$ of 0.03 $\mu$M. It is evident that the 3-hydroxyphenyl derivative **6b** represented the most promising suppression activity against the wild and the mutant form T790M of EGFR compared with the reference standards erlotinib and AZD9291 (Figure 4). The obtained results were in agreement with the data of cytotoxicity evaluation. The docking study correlated the enhanced activity of **6b** to its hydroxyl oxygen that was a site for H-bonding in the active regions of $EGFR^{WT}$ and $EGFR^{T790M}$, while the *N*-phenyl moiety increased the hydrophobic interaction with the target enzyme.

Moreover, it could be detected that all the compounds exhibited more potent inhibitory activity against the mutant form $EGFR^{T790M}$ over the wild-type form $EGFR^{WT}$, which can overcome the resistance problem to EGFR-TKIs that develops due to the T790M mutation of the EGFR gene.

*2.2.3. In Vivo Inhibition of p53 Ubiquitination.* The p53 protein plays a crucial role in the regulation of cancer development through its action as a suppressing molecule that binds to E3 ubiquitin ligase, thus inhibiting its role as a


https://doi.org/10.1021/acsomega.1c06836
ACS Omega 2022, 7, 7155−7171

transcription activator.[98,99] Therefore, interfering with p53 binding on E3 ligase can interfere with tumor development and progression. Following the reported methodology,[99] the obtained results exhibited that the compounds **5**−**7** showed moderate inhibitory actions toward *in vivo* p53 ubiquitination compared to the reference diphenyl imidazole (DPI). According to Table 4, compounds **5a**−**c** have recorded $IC_{50}$ values greater than the reference drug of $IC_{50}$'s of 0.68, 0.62, and 0.60 nM and $IC_{50DPI}$ of 0.26 ± 0.005 nM. A higher potency was reported by the compounds **6a**−**c** and **7** affording $IC_{50}$ values ranging from 0.59 to 0.48 nM. Accordingly, these results revealed that the tested analogues can still act as p53 ubiquitination inhibitors and thus can intervene with cancer cell growth and development.

**Table 4. $IC_{50}$ Values Obtained Due to *In Vivo* p53 Ubiquitination Inhibition of MCF-7 Cells**

| | $IC_{50}$ (mean ± SEM) (nM) |
|---|---|
| compound no. | p53 ubiquitination |
| DPI | 0.26 ± 0.005 |
| **5a** | 0.68 ± 0.01 |
| **5b** | 0.62 ± 0.05 |
| **5c** | 0.60 ± 0. 03 |
| **6a** | 0.59 ± 0. 01 |
| **6b** | 0.50 ± 0.05 |
| **6c** | 0.48 ± 0.02 |
| 7 | 0.48 0 ± 0.05 |

**2.3. Molecular Modeling Study on $EGFR^{WT}$ and Mutant $EGFR^{T790M}$.** In the current docking simulation, the potent kinase inhibitors **5**−**7** were selected based on the potency and scaffold type to correlate the structure−activity relationship with their behavior and the possible binding interactions within the active sites of $EGFR^{WT}$ and mutant $EGFR^{T790M}$. Thus, the domains of $EGFR^{WT}$ and mutant $EGFR^{T790M}$ kinase complexed with erlotinib and AZD9291 (PDB ID: 1M17 and 6JX0)[100,101] were downloaded from the Protein Data Bank. The docking calculations were done using MOE-Dock (Molecular Operating Environment) software version 2014.0901.[102,103] At the beginning, redocking of the native ligands (erlotinib and AZD9291) was achieved within their own binding sites of $EGFR^{WT}$ and $EGFR^{T790M}$, giving energy scores −11.40 and −12.66 kcal/mol with RMDS values (root mean square deviation) of 0.91 and 1.02 Å, respectively. It was noted that the compounds **5**−**7** approximately displayed similar binding poses with promising energy scores that are depicted in Tables 5 and 6.

All the screened derivatives **5**−**7** afforded H-bonding with the key amino acids **Met769** and **Met793** within the active sites of $EGFR^{WT}$ and mutant $EGFR^{T790M}$ kinases like the original ligands erlotinib and AZD9291, respectively. Furthermore, the existence of 1,2,4-triazoles in compounds **5** and **6**, in addition to the 1,3,5-triazine moiety in compound **7**, potentiates fixation within the binding pockets of $EGFR^{WT}$ and $EGFR^{T790M}$ enzymes through extra H-bonding with **Lys721** and **Met793**, respectively.

By focusing upon compound **6b** as the most active inhibitor, it fulfilled the key interactions in the active site of $EGFR^{WT}$ with energy score −10.88 kcal/mol, where hydrogen bonding was established between N-2 of the 1,2,4-triazole moiety and the side chain of **Lys721** (distance: 3.63 Å), as well as the Pi-cation interaction of the phenolic ring with the **Val702** residue.

**Table 5. Docking Study of Compounds 5−7 within $EGFR^{WT}$ (PDB Code: 1M17) Using MOE Software Version 2014.0901**

| compd. no. | docking score (kcal/mol) | amino acid residues (bond length Å) | atoms of compound | type of bond |
|---|---|---|---|---|
| erlotinib | −11.40 | Met769(2.70) | N1(quinazoline) | H-acc |
| **5a** | −10.15 | Lys721(2.92) | N-4(1,2,4-triazole) | H-acc |
| | | Met769(2.75) | N(thiazole) | H-acc |
| **5b** | −10.32 | Lys721(2.65) | N-4(1,2,4-triazole) | H-acc |
| | | Met769(2.95) | N(linker NH) | H-acc |
| **5c** | −9.85 | Lys702 | phenol | arene-cation |
| | | Lys721(2.75) | N-4(1,2,4-triazole) | H-acc |
| | | Met769(2.60) | O(OH) | H-acc |
| **6a** | −10.50 | Lys721(3.22) | N-2(1,2,4-triazole) | H-acc |
| | | Met769(2.88) | N(thiazole) | H-acc |
| **6b** | −10.88 | Val702 | phenol | arene-cation |
| | | Lys721(3.63) | N-2(1,2,4-triazole) | H-acc |
| | | Met769(3.27) | O(OH) | H-acc |
| **6c** | −10.25 | Lys721(3.20) | N-2(1,2,4-triazole) | H-acc |
| | | Met769(3.60) | $O(NO_2)$ | H-acc |
| 7 | −10.36 | Lys721(2.70) | N-3(1,3,5-triazine) | H-acc |
| | | Met769(2.80) | N(thiazole) | H-acc |

The presence of the H-bond acceptor between the hydroxyl oxygen and the backbone of the key amino acid **Met769** improved the fitting within the active site of the enzyme (distance: 3.27 Å) (Figure 5).

Regarding the docking of **6b** within the ATP-binding pocket of $EGFR^{T790M}$ allowing energy score −13.27 kcal/mol, it was found that N-2 of the 1,2,4-triazole scaffold and the NH linker at position-5 played a vital role in the binding through a bidentate hydrogen-bonded interaction with the backbone of the hinge **Met793** (distance: 3.65 and 3.06 Å, respectively). Moreover, the phenolic ring shared fixation through Pi-cation interaction with **Leu718** (Figure 6).

The analysis of the docking results demonstrated that compound **6b** with the highest $EGFR^{WT}$ and $EGFR^{T790M}$ inhibitory activities adopted good binding mode through its characterized structure of the 1,2,4-triazole core and the phenolic ring linked via the NH group forming hydrophilic and hydrophobic interactions.

## 3. CONCLUSIONS

A new set of benzimidazole, 1,2,4-triazole, and 1,3,5-triazine derivatives was designed and synthesized using microwave irradiation. The cytotoxic activity of all the new analogues was evaluated against a panel of four human cancer cell lines—HepG-2, PC-3, MCF-7, and A-549—in addition to the normal peripheral blood mononuclear cells (PBMCs) using doxorubicin and erlotinib as standard drugs. The gained results represented the significant selective cytotoxicity of some of the examined derivatives against MCF-7 and A-549 cell lines. The most potent cytotoxic activity against MCF-7 cells was revealed by the *N*-phenyl-1,2,4-triazole analogues **6a**−**c**, exhibiting $IC_{50}$ values ranging from 1.29 to 4.30 $\mu$M that



https://doi.org/10.1021/acsomega.1c06836
ACS Omega 2022, 7, 7155−7171

**Table 6. Docking Study of Compounds 5−7 within EGFR$^{T790M}$ (PDB Code: 6JX0) Using MOE Software Version 2014.0901**

| compd. no. | docking score (kcal/mol) | amino acid residues (bond length Å) | atoms of compound | type of bond |
|---|---|---|---|---|
| AZD9291 | −12.66 | Val726 | indole | arene-cation |
| | | Met793(2.88) | N-1(pyrimidine) | H-acc |
| | | Asp800(3.27) | N(N(CH$_3$)$_2$) | H-don |
| **5a** | −11.20 | Leu718 | thiazole | arene-cation |
| | | Met793(2.95) | N-1(1,2,4-triazole) | H-don |
| | | Met793(2.80) | N(linker NH) | H-don |
| **5b** | −10.74 | Met793(3.15) | N-1(1,2,4-triazole) | H-don |
| | | Met793(3.00) | N(linker NH) | H-don |
| **5c** | −10.70 | Leu718 | phenol | arene-cation |
| | | Met793(2.77) | N-1(1,2,4-triazole) | H-don |
| | | Met793(2.60) | N(linker NH) | H-don |
| **6a** | −11.45 | Leu718 | thiazole | arene-cation |
| | | Met793(3.55) | N-4(1,2,4-triazole) | H-acc |
| | | Met793(3.26) | N(linker NH) | H-don |
| **6b** | −11.75 | Leu718 | phenol | arene-cation |
| | | Met793(3.65) | N-4(1,2,4-triazole) | H-acc |
| | | Met793(3.06) | N(linker NH) | H-don |
| **6c** | −11.35 | Leu718 | 2-Cl-4-NO$_2$-C$_6$H$_3$ | arene-cation |
| | | Met793(3.22) | N-4(1,2,4-triazole) | H-acc |
| | | Met793(2.90) | N(linker NH) | H-don |
| **7** | −11.20 | Leu718 | thiazole | arene-cation |
| | | Met793(3.15) | N-1(1,3,5-triazine) | H-don |
| | | Met793(2.85) | N(linker NH) | H-don |

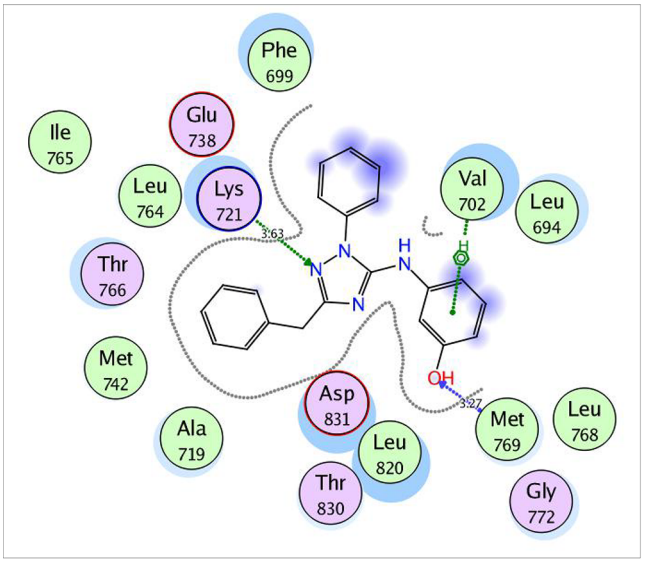


A

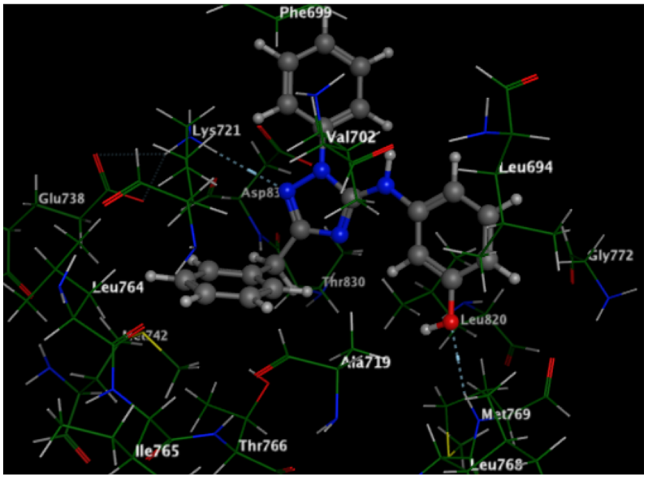


B

**Figure 5.** 2D and 3D schematic binding interactions (A and B) of compound **6b** into EGFR$^{WT}$ (PDB code: 1M17) using the MOE software.

were evidently near those of the reference compounds (doxorubicin and erlotinib) of IC$_{50}$ of 4.17 and 4.16 $\mu$M, respectively. Moreover, A-549 cancer cells represented about 1.3−2.6-folds more sensitivity against the latter derivatives than that against doxorubicin and approximately equal sensitivity to that obtained against erlotinib exhibiting IC$_{50}$'s ranging from 3.18 to 5.80 $\mu$M and IC$_{50;\ \text{doxorubicin, erlotinib}}$ of 8.20 and 3.76 $\mu$M, respectively. On the other hand, both MCF-7 and A-549 cell lines displayed an equipotent or a slightly less sensitivity against the 1,2,4-triazole analogues **5a−c** and the 1,3,5-triazinone **7** than that against the reference drugs displaying IC$_{50}$'s ranging from 4.18 to 5.42 and 7.43 to 12.30 $\mu$M, respectively. With the exception of compounds **8c** and **8d** that were as potent as doxorubicin against the A-549 cell line, an observable decrease in the cytotoxic activity was detected in the 1,3,5-triazin-2-thione derivatives **8** against both MCF-7 and A-549 cell lines with IC$_{50}$ values of 10.31−25.46 and 37.21−25.46 $\mu$M, respectively. Moreover, moderate to weak antiproliferative activity against hepatocellular carcinoma (HepG-2) and prostate carcinoma (PC-3) cell lines was detected by the tested compounds. All the tested derivatives represented low cytotoxicity against the normal PBMC cell line with IC$_{50}$ values <100 $\mu$M, confirming the safety margin of the new derivatives.

Furthermore, the new target compounds showing the most promising anticancer activity (**5**, **6**, and **7**) were evaluated as *in vitro* EGFR$^{WT}$ and EGFR$^{T790M}$ inhibitors compared to the reference drugs erlotinib and AZD9291. Generally, the target derivatives represented a promising inhibitory effect against EGFR$^{WT}$ and EGFR$^{T790M}$ with more potency against the mutant form EGFR$^{T790M}$, which is a good property to overcome the EGFR-TKI resistance problem. Also, derivative **6b** represented the most potent suppression effect against both EGFR$^{WT}$ and EGFR$^{T790M}$.

Moreover, compounds **5−7** down-regulated the oncogenic parameter p53 ubiquitination, representing approximately an equivalent suppression potency to the reference diphenyl imidazole (DPI). The docking simulation study was performed for the promising inhibitors **5−7**, giving energy scores of −11.40 and −12.66 kcal/mol with RMDS values of 0.91 and 1.02 Å, respectively. Compound **6b** was chosen as a representative example to find out the binding modes of the compound in the active pocket of EGFR$^{WT}$ and the mutant



https://doi.org/10.1021/acsomega.1c06836
ACS Omega 2022, 7, 7155−7171

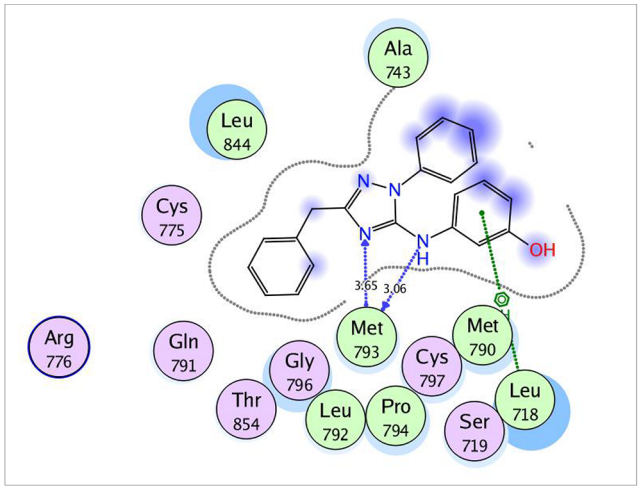


A

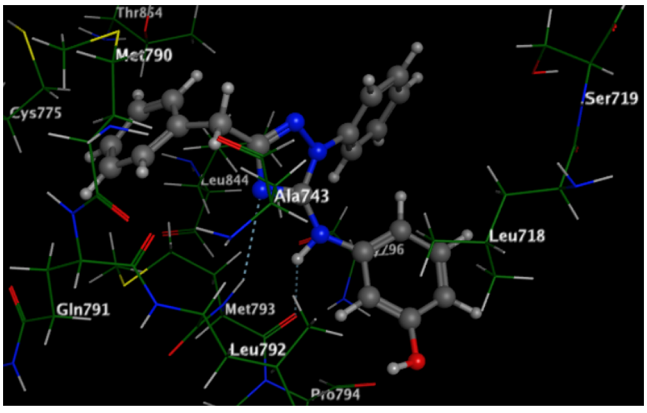


B

**Figure 6.** 2D and 3D schematic binding interactions (A and B) of compound **6b** into EGFR$^{T790M}$ (PDB code: 6JX0) using the MOE software.

EGFR$^{T790M}$. It adopted promising binding interactions with the active sites of the tested proteins through its 1,2,4-triazole scaffold and the phenolic ring linked via the NH group forming various hydrophilic and hydrophobic interactions in the active pocket of the wild EGFR$^{WT}$ and its mutated form EGFR$^{T790M}$.

As an overview on the obtained results, it has been investigated that **6b** is a new potent antitumor agent exhibiting a safety profile against the normal cells as well as a promising inhibitory impact against EGFR$^{WT}$ and EGFR$^{T790M}$. These advantages together indicated that **6b** could be considered as an auspicious lead compound for the future evolution of new more potent anticancer candidates inhibiting EGFR mutations.

## 4. EXPERIMENTAL SECTION

**4.1. Chemistry.** The instruments used for measuring the melting points, spectral data (IR, mass, $^1$H NMR and $^{13}$C NMR, X-ray) and elemental analysis are provided in detail in the Supplementary Information.

*4.1.1. Synthesis of the Thiourea Derivatives* ***2a–e****.* A mixture of 2-phenylacetyl isothiocyanate (**1**) (0.01 mol) and different amine derivatives, namely, isopropylamine, 2-aminothiazole, *o*-phenylenediamine, *m*-aminophenol, and *o*-chloro-*p*-nitroaniline (0.01 mol) in dry acetonitrile (20 mL), was stirred at room temperature for 3 h. The solid product obtained was filtered and recrystallized from ethanol to give the corresponding thiourea derivatives **2a–e**, respectively.

*4.1.1.1. N-(Isopropylcarbamothioyl)-2-phenylacetamide (**2a**).* Pale yellow crystals; yield 98%, m.p. 70–72 °C. IR (KBr) ($\upsilon$, cm$^{-1}$): 3287, 3192 (NH), 3064 (CH$_{arom}$), 2974, 2930, 2875 (CH$_{aliph}$), 1660 (C=O), 1639 (C=N), 1173 (C=S); $^1$H NMR (DMSO-$d_6$) $\delta$: 1.06 (d, 6H, CH$_3$), 3.43 (s, 2H, CH$_2$-ph), 3.80–3.84 (m, 1H, CH(CH$_3$)$_2$), 7.20–7.33 (m, 5H, Ar-H, $J$ = 7.27 Hz), 7.96 (br.s, 1H, NH, D$_2$O exchangeable), 11.35 (br.s, 1H, NH, D$_2$O exchangeable); $^{13}$C NMR (DMSO-$d_6$) $\delta$: 22.85, 42.89, 46.86, 126.70, 128.63, 129.33, 137.11, 169.56, 179.12; MS (70 eV) $m/z$ (%): 236 (M$^+$, 19). Anal. calcd for $C_{12}H_{16}N_2Os$ (236.33): C, 60.99; H, 6.82; N, 11.85. Found: C, 60.86; H, 7.12; N, 11.67.

*4.1.1.2. 2-Phenyl-N-(thiazol-2-ylcarbamothioyl) Acetamide (**2b**).* Pale brown crystals; yield 90%, m.p. 242–244 °C; IR (KBr) ($\upsilon$, cm$^{-1}$): 3267, 3171 (NH), 3080 (CH$_{arom}$), 2947, 2893 (CH$_{aliph}$), 1685 (C=O), 1567 (C=N), 1166 (C=S); $^1$H NMR (DMSO-$d_6$) $\delta$: 3.78 (s, 2H, CH$_2$-ph), 7.20–7.26 (d, 2H, thiazole-H$_4$, H$_5$), 7.34–7.63 (m, 5H, Ar-H, $J$ = 7.67 Hz), 8.01 (br.s, 1H, NH, D$_2$O exchangeable), 12.37 (br.s, 1H, NH, D$_2$O exchangeable); $^{13}$C NMR (DMSO-$d_6$) $\delta$: 42.12, 113.96, 130.36, 138.06, 127.27, 128.88, 129.70, 135.47, 158.46, 169.62; MS (70 eV) $m/z$ (%): 277 (M$^+$, 18). Anal. calcd for $C_{12}H_{11}N_3OS_2$ (277.36): C, 51.97; H, 4.00; N, 15.15. Found: C, 51.62; H, 3.87; N, 14.86.

*4.1.1.3. N-((2-Aminophenyl)carbamothioyl)-2-phenylacetamide (**2c**).* Yellow crystals; yield 94%; m.p. 188–190 °C; IR (KBr) ($\upsilon$, cm$^{-1}$): 3370, 3327, 3135 (NH, NH$_2$), 3030 (CH$_{arom}$), 2950, 2830 (CH$_{aliph}$), 1690 (C=O), 1670 (C=N), 1167 (C=S); $^1$H NMR (DMSO-$d_6$) $\delta$: 3.82 (s, 2H, CH$_2$-ph), 5.01 (br.s, 2H, NH$_2$, D$_2$O exchangeable), 6.57–7.80 (m, 9H, Ar-H, $J$ = 7.10 Hz), 11.63 (br.s, 1H, NH, D$_2$O exchangeable), 12.13 (br.s, 1H, NH, D$_2$O exchangeable); $^{13}$C NMR (DMSO-$d_6$) $\delta$: 42.80, 109.96, 116.32, 127.40, 127.67, 128.87, 129.90, 132.80, 134.45, 143.70, 173.30, 180.67; MS (70 eV) $m/z$ (%): 285 (M$^+$, 14). Anal. calcd for $C_{15}H_{15}N_3Os$ (285.37): C, 63.13; H, 5.30; N, 14.73. Found: C, 63.09; H, 5.27; N, 14.69.

*4.1.1.4. N-((3-Hydroxyphenyl)carbamothioyl)-2-phenylacetamide (**2d**).* Beige powder; yield 98%, m.p. 260–262° C; IR (KBr) ($\upsilon$, cm$^{-1}$): 3304 (OH), 3246, 3199 (NH), 3063 (CH$_{arom}$), 2906, 2820 (CH$_{aliph}$), 1684 (C=O), 1609 (C=N), 1146 (C=S); $^1$H NMR (DMSO-$d_6$) $\delta$: 3.83 (s, 2H, CH$_2$-ph), 6.67–7.36 (m, 9H, Ar-H, $J$ = 7.05 Hz), 9.66 (br.s, 1H, OH, D$_2$O exchangeable), 11.67 (br.s, 1H, NH, D$_2$O exchangeable), 12.41 (br.s, 1H, NH, D$_2$O exchangeable); $^{13}$C NMR (DMSO-$d_6$) $\delta$: 39.94, 111.28, 113.86, 114.90, 127.48, 128.93, 129.95, 134.74, 139.13, 157.98, 173.75, 178.85; MS (70 eV) $m/z$ (%): 286 (M$^+$, 39). Anal. calcd for $C_{15}H_{14}N_2O_2S$ (286.35): C, 62.92; H, 4.93; N, 9.78. Found: C, 61.21; H, 5.21; N, 9.67.

*4.1.1.5. N-((2-Chloro-4-nitrophenyl)carbamothioyl)-2-phenylacetamide (**2e**).* Yellow powder; yield 97%, m.p. 105–107° C; IR (KBr) ($\upsilon$, cm$^{-1}$): 3275, 3198 (NH), 3091, 3009 (CH$_{arom}$), 2921, 2815 (CH$_{aliph}$), 1684 (C=O), 1625 (C=N), 1147 (C=S); $^1$H NMR (DMSO-$d_6$) $\delta$: 3.86 (s, 2H, CH$_2$-ph), 6.84–7.35 (m, 5H, Ar-H, $J$ = 7.69 Hz), 7.94–8.63 (m, 3H, Ar-H, $J$ = 7.31, 7.63 Hz), 12.11 (br.s, 1H, NH, D$_2$O exchangeable), 12.85 (br.s, 1H, NH, D$_2$O exchangeable); $^{13}$C NMR (DMSO-$d_6$) $\delta$: 42.77, 120.43, 122.98, 125.13, 126.92, 130.02, 134.44, 136.36, 145.35, 151.83, 173.98, 180.07; MS (70 eV) $m/z$ (%): 349 (M$^+$, 29). Anal. calcd for


https://doi.org/10.1021/acsomega.1c06836
ACS Omega 2022, 7, 7155–7171

$C_{15}H_{12}ClN_3O_3S$ (349.79): C, 51.51; H, 3.46; N, 12.01. Found: C, 51.13; H, 3.67; N, 11.69.

*4.1.2. Synthesis of N-(1H-Benzo[d]imidazol-2-yl)-2-phenylacetamide (**3**).* A solution of compound **2c** (2.85 g; 0.01 mol) in ethyl alcohol (5 mL) was irradiated under MW for 2 min at 80 °C. After cooling at room temperature, the precipitate was filtered and recrystallized from ethanol to give the corresponding compound **3**.

White crystals; yield (80%); m.p. 206−208 °C; IR (KBr) ($\upsilon$, $cm^{-1}$): 3200, 3128 (NH), 3067, 3028 ($CH_{arom}$), 2910, 2820 ($CH_{alkyl}$), 1670 (C═O), 1512 (C═N); $^1H$ NMR (DMSO-$d_6$) $\delta$: 3.76 (s, 2H, $CH_2$-ph), 6.57−7.80 (m, 9H, Ar-H, $J$ = 7.28, 7.68 Hz), 11.74 (br. s, 1H, NH, $D_2O$ exchangeable), 12.11 (br.s, 1H, NH, $D_2O$ exchangeable); $^{13}C$ NMR (DMSO-$d_6$) $\delta$: 40.06, 116.32, 116.50, 127.43, 128.87, 128.90, 129.88, 130.01, 134,70, 143.66, 173.30; MS (70 eV) $m/z$ (%): 251 ($M^+$, 5). Anal. calcd for $C_{15}H_{13}N_3O$ (251.29): C, 71.70; H, 5.21; N, 16.72. Found: C, 71.53; H, 5.03; N, 16.48.

*4.1.3. Synthesis of 2-Phenyl-N-(2-phenyl-1H-enzo[d]-imidazole-1-carbonothioyl)acetamide (**4**).* A mixture of compound **2c** (2.85 g; 0.01 mol) and benzoyl chloride (0.01 mol) in ethyl alcohol (5 mL) was irradiated under MW radiation for 3 min at 80 °C, and then it was treated with cold water. The formed solid was filtered, washed with water, dried, and recrystallized from ethanol to give compound **4**. Yellow crystals; yield 96%, m.p. 260−280 °C; IR (KBr) ($\upsilon$, $cm^{-1}$): 3219 (NH), 3063, 3026 ($CH_{arom}$), 2960, 2820 ($CH_{aliph}$), 1699 (C═O), 1625 (C═N), 1266 (C═S); $^1H$ NMR (DMSO-$d_6$) $\delta$: 3.91 (s, 2H, $CH_2$-ph),7.36−8.24 (m, 14H, Ar-H, $J$ = 7.48, 7.94 Hz), 12.78 (br.s, 1H, NH, $D_2O$ exchangeable); $^{13}C$ NMR (DMSO-$d_6$) $\delta$: 40.32, 114.05, 125.02, 128.92, 129.09, 129.37, 129.60, 129.87, 129.98, 131.99, 134.18, 144.71, 166.53, 167.0; MS (70 eV) $m/z$ (%): 371 ($M^+$, 68). Anal. calcd for $C_{22}H_{17}N_3OS$ (371.46): C, 71.14; H, 4.61; N, 11.31. Found: C, 71.11; H, 4.58; N, 11.28.

*4.1.4. Synthesis of 1,2,4-Triazole Derivatives **5a−c** and **6a−c**.* A mixture of **2a**, **b**, and **d** (0.01 mol) and hydrazine hydrate or phenyl hydrazine (0.01 mol) was heated in MW for 2−10 min at 120−150 °C in the presence of DMF as a solvent. After cooling, the reaction mixture was poured into ice water. The obtained precipitate was filtered and recrystallized from ethanol to give corresponding products **5a−c** and **6a−c**, respectively.

*4.1.4.1. 5-Benzyl-N-isopropyl-4H-1,2,4-triazol-3-amine (**5a**).* White needles, yield 98%, m.p. 84−86 °C; IR (KBr) ($\upsilon$, $cm^{-1}$): 3288 (NH), 3065, 3029 ($CH_{arom}$), 2975, 2930, 2874 ($CH_{aliph}$), 1639 (C═N); $^1H$ NMR (DMSO-$d_6$) $\delta$: 1.06 (d, 6H, $CH_3$), 3.39 (m, 1H, CH), 3.82 (s, 2H, $CH_2$-ph), 7.21 (br. s, 1H, NH, $D_2O$ exchangeable), 7.22−7.31 (m, 5H, Ar-H, $J$ = 7.26, 7.30 Hz), 7.95 (br. s, 1H, NH, $D_2O$ exchangeable); $^{13}C$ NMR (DMSO-$d_6$) $\delta$: 22.86, 39.84, 42.90, 126.69, 128.62, 129.34, 137.13, 155.40, 169.51; MS (70 eV) $m/z$ (%): 216 ($M^+$, 69). Anal. calcd for $C_{12}H_{16}N_4$ (216.28): C, 66.64; H, 7.46; N, 25.90. Found: C, 66.60; H, 7.40; N, 25.88.

*4.1.4.2. N-(5-Benzyl-4H-1,2,4-triazol-3-yl)thiazol-2-amine (**5b**).* White powder; yield 96%, m.p. 220−222 °C; IR (KBr) ($\upsilon$, $cm^{-1}$): 3199 (NH), 3056, 3020 ($CH_{arom}$), 2922, 2850 ($CH_{aliph}$), 1663 (C═N); $^1H$ NMR (DMSO-$d_6$) $\delta$: 3.84 (s, 2H, $CH_2$-ph), 7.16, 7.25 (2d, 2H, thiazole-$H_4$, $H_5$), 7.30−7.32 (m, 5H, Ar-H, $J$ = 7.17, 7.23, 7.30 Hz), 7.45 (br. s, 1H, NH, $D_2O$ exchangeable), 12.31 (br. s, 1H, NH, $D_2O$ exchangeable); $^{13}C$ NMR (DMSO-$d_6$) $\delta$: 42.07, 114.09, 127.39, 128.95, 129.64, 135.26, 138.04, 158.37, 159.04, 169.86; MS (70 eV) $m/z$ (%): 257 ($M^+$, 18). Anal. calcd for $C_{12}H_{11}N_5S$ (257.31): C, 56.01; H, 4.31; N, 27.22. Found: C, 55.97; H, 4.29; N, 26.98.

*4.1.4.3. 3-((5-Benzyl-4H-1,2,4-triazol-3-yl)amino)phenol (**5c**).* Pale brown crystals; yield 86%, m.p. 110−112 °C; IR (KBr) ($\upsilon$, $cm^{-1}$): 3328 (OH), 3270, 3145 (NH), 3086, 3027 ($CH_{arom}$), 2964, 2840 ($CH_{aliph}$), 1662 (C═N). $^1H$ NMR (DMSO-$d_6$) $\delta$: 3.50 (s, 2H, $CH_2$-ph), 6.62−7.31 (m, 9H, Ar-H, $J$ = 7.37, 7.74 Hz), 8.10 (br. s, 1H, NH, $D_2O$ exchangeable), 9.30 (br. s, 1H, NH, $D_2O$ exchangeable), 9.60 (br. s, 1H, OH, $D_2O$ exchangeable); $^{13}C$ NMR (DMSO-$d_6$) $\delta$: 38.83, 102.52, 110.41, 115.98, 125.06, 128.07, 130.15, 136.49, 143.80, 156.12, 159.54, 160.08, 165.13; MS (70 eV) $m/z$ (%): 266 ($M^+$, 81). Anal. calcd for $C_{15}H_{14}N_4O$ (266.30): C, 67.65.17; H, 5.30; N, 21.04. Found: C, 67.40; H, 5.18; N, 20.98.

*4.1.4.4. N-(3-Benzyl-1-phenyl-1H-1,2,4-triazol-5-yl)-thiazol-2-amine (**6a**).* Brown powder, yield 95%, m.p. 170−172 °C; IR (KBr) ($\upsilon$, $cm^{-1}$): 3285 (NH), 3084, 3026 ($CH_{arom}$), 2919 ($CH_{aliph}$), 1664 (C═N). $^1H$ NMR (DMSO-$d_6$) $\delta$: 3.50 (s, 2H, $CH_2$-ph), 6.67, 7.10 (2d, 2H, thiazole-$H_4$, $H_5$), 7.26−7.74 (m, 10H, Ar-H, $J$ = 7.10, 7.37 Hz), 10.23 (br. s, 1H, NH, $D_2O$ exchangeable); $^{13}C$ NMR (DMSO-$d_6$) $\delta$: 40.08, 112.49, 126.99, 128.53, 128.71, 128.75, 129.12, 129.48, 129.83, 136.38, 149.75, 170.43; MS (70 eV) $m/z$ (%): 333 ($M^+$, 10). Anal. calcd for $C_{18}H_{15}N_5S$ (333.41): C, 64.84; H, 4.53; N, 21.01. Found: C, 64.81; H, 4.50; N, 20.97.

*4.1.4.5. 3-((3-Benzyl-1-phenyl-1H-1,2,4-triazol-5-yl)-amino)phenol (**6b**).* White powder, yield 85%, m.p. 158−160 °C; IR (KBr) ($\upsilon$, $cm^{-1}$): 3285 (OH), 3206 (NH), 3084, 3027 ($CH_{arom}$), 2915 ($CH_{aliph}$), 1664 (C═N); $^1H$ NMR (DMSO-$d_6$) $\delta$: 3.51 (s, 2H, $CH_2$-ph), 6.66−7.73 (m, 14H, Ar-H, $J$ = 6.68, 7.16 Hz), 9.09 (br. s, 1H, NH, $D_2O$ exchangeable), 9.90 (br. s, 1H, OH, $D_2O$ exchangeable); $^{13}C$ NMR (DMSO-$d_6$) $\delta$: 40.94, 112.52, 118.98, 127.02, 128.77, 129.15, 129.49, 136.36, 149.73, 170.51; MS (70 eV) $m/z$ (%): 342 ($M^+$, 25). Anal. calcd for $C_{21}H_{18}N_4O$ (342.39): C, 73.67; H, 5.30; N, 16.36. Found: C, 73.96; H, 5.15; N, 15.96.

*4.1.4.6. 3-Benzyl-N-(2-chloro-4-nitrophenyl)-1-phenyl-1H-1,2,4-triazol-5-amine (**6c**).* White powder, yield 89%, m.p. 180−182 °C; IR (KBr) ($\upsilon$, $cm^{-1}$): 3284 (NH), 3084, 3026 ($CH_{arom}$), 2915, 2840 ($CH_{aliph}$), 1664 (C═N); $^1H$ NMR (DMSO-$d_6$) $\delta$: 4.23 (s, 2H, $CH_2$-ph), 6.67−7.60 (m, 10H, Ar-H, $J$ = 8.18 Hz), 8.22−8.38 (d, 2H, Ar-H, $J$ = 7.59 Hz), 9.22 (s, 1H, Ar-H), 9.90 (br. s, 1H, NH, $D_2O$ exchangeable); $^{13}C$ NMR (DMSO-$d_6$) $\delta$: 40.39, 118.43, 122.26, 124.83, 126.12, 128.04, 136.14, 138.36, 139.25, 151.83, 158.32, 162.15; MS (70 eV) $m/z$ (%): 406 ($M^+$, 49). Anal. calcd for $C_{21}H_{16}ClN_5O_2$ (405.84): C, 62.15; H, 3.97; N, 17.26. Found: C, 62.11; H, 3.95; N, 17.24.

*4.1.5. Synthesis of 4-Benzyl-6-(thiazol-2-ylamino)-1,3,5-triazin-2(5H)-one (**7**).* A mixture of **2b** (2.77 g; 0.01 mol) and urea (0.60 g; 0.01 mol) in DMF (5 mL) was heated under MW irradiation for 5 min at 130 °C. After cooling to room temperature, the reaction mixture was poured onto ice. The obtained precipitate was filtered and recrystallized from ethanol to give the corresponding compound **7**.

Pale brown crystals, yield 97%, m.p. 242−244 °C IR (KBr) ($\upsilon$, $cm^{-1}$): 3206 (NH), 3081 ($CH_{arom}$), 2950, 2885 ($CH_{aliph}$), 1686 (C═O), 1626 (C═N); $^1H$ NMR (DMSO-$d_6$) $\delta$: 3.77 (s, 2H, $CH_2$-ph), 6.93−7.47 (m, 7H, Ar-H, $J$ = 7.32 Hz), 11.19 (br. s, 1H, NH, $D_2O$ exchangeable), 12.35 (br. s, 1H, NH, $D_2O$ exchangeable); $^{13}C$ NMR (DMSO-$d_6$) $\delta$: 40.13, 113.96, 127.27, 128.88, 129.69, 135.47, 138.10150.41, 158.44, 169.63; MS (70 eV) $m/z$ (%): 285 ($M^+$, 32). Anal. calcd for


https://doi.org/10.1021/acsomega.1c06836
ACS Omega 2022, 7, 7155−7171

$C_{13}H_{11}N_5OS$ (285.32): C, 54.72; H, 3.89; N, 24.55. Found: C, 54.70; H, 3.86; N, 24.51.

*4.1.6. Synthesis 1,3,5-Triazin-2-thione Derivatives* ***8a−d.*** An equimolar ratio of **2a**, **b**, **d**, and **e** (0.01 mol) and thiourea (0.74 g; 0.01 mol) in DMF (5 mL) was heated in MW for 2−10 min at 130−150 °C. After cooling to room temperature, the reaction mixture was poured onto ice. The obtained precipitate was filtered and recrystallized from ethanol to give corresponding products **8a−d**, respectively.

*4.1.6.1. 6-Benzyl-4-(isopropylimino)-3,4-dihydro-1,3,5-triazine-2(1H)-thione (**8a**).* Pale brown crystals, yield 96%, m.p. 260−262 °C; IR (KBr) ($\upsilon$, $cm^{-1}$): 3289, 3110 (NH), 3065, 3030 ($CH_{arom}$), 2975, 2930, 2875 ($CH_{aliph}$), 1639 (C═N), 1175 (C═S); $^1H$ NMR (DMSO-$d_6$) $\delta$: 1.05 (d, 6H, $CH_3$), 3.36 (m, 1H, CH), 3.82 (s, 2H, ph-$CH_2$), 7.21−7.30 (m, 5H, Ar-H, $J$ = 7.12 Hz), 7.96 (br. s, 1H, NH, $D_2O$ exchangeable), 11.35 (br. s, 1H, NH, $D_2O$ exchangeable); $^{13}C$ NMR (DMSO-$d_6$) $\delta$: 22.85, 40.15, 42.88, 126.71, 128.60, 128.64, 129.27, 129.33, 132.66, 137.11, 169.56; MS (70 eV) $m/z$ (%): 260 ($M^+$, 29). Anal. calcd for $C_{13}H_{16}N_4S$ (260.36): C, 59.97; H, 6.19; N, 21.52. Found: C, 59.93; H, 6.15; N, 21.49.

*4.1.6.2. 6-Benzyl-4-(thiazol-2-ylimino)-3,4-dihydro-1,3,5-triazine-2(1H)-thione (**8b**).* Brown crystals, yield 97%, m.p. 151−153 °C; IR (KBr) ($\upsilon$, $cm^{-1}$): 3220 (NH), 3072, 3028 ($CH_{arom}$), 2918, 2862 ($CH_{aliph}$), 1620 (C═N), 1164 (C═S); $^1H$ NMR (DMSO-$d_6$) $\delta$: 3.77 (s, 2H, $CH_2$-ph), 7.20−7.28 (m, 5H, Ar-H, $J$ = 7.34 Hz), 7.35−7.48 (2d, 2H, thiazole-$H_4$, $H_5$, $J$ = 7.20, 7.27 Hz), 8.33 (br. s, 1H, NH, $D_2O$ exchangeable), 12.35 (br. s, 1H, NH, $D_2O$ exchangeable); $^{13}C$ NMR (DMSO-$d_6$) $\delta$: 40.06, 113.97, 127.28, 128.88, 129.69, 135.47, 138.11, 158.42, 169.62; MS (70 eV) $m/z$ (%): 301 ($M^+$, 42). Anal. calcd for $C_{13}H_{11}N_5S_2$ (301.39): C, 51.81; H, 3.68; N, 23.24. Found: C, 51.78; H, 3.79; N, 23.22.

*4.1.6.3. 6-Benzyl-4-((3-hydroxyphenyl)imino)-3,4-dihydro-1,3,5-triazine-2(1H)-thione (**8c**).* Brown crystals, yield 92%, m.p. 147−149 °C. IR (KBr) ($\upsilon$, $cm^{-1}$): 3357 (OH), 3216 (NH), 3050, 3022 ($CH_{arom}$), 2925, 2815 ($CH_{aliph}$), 1603(C═N), 1177 (C═S); $^1H$ NMR (DMSO-$d_6$) $\delta$: 3.51 (s, 2H, ph-$CH_2$), 6.65−7.76 (m, 9H, Ar-H, $J$ = 6.68, 7.28 Hz), 8.73 (br. s, 1H, NH, $D_2O$ exchangeable), 9.09 (br. s, 1H, NH, $D_2O$ exchangeable), 9.90 (br. s, 1H, OH, $D_2O$ exchangeable); $^{13}C$ NMR (DMSO-$d_6$) $\delta$: 41.90, 112.20, 113.65, 114.65, 127.40, 128.95, 129.90, 134.74, 139.13, 150.42, 156.90, 170.75; MS (70 eV) $m/z$ (%): 310 ($M^+$, 32). Anal. calcd for $C_{16}H_{14}N_4OS$ (310.37): C, 61.92; H, 4.55; N, 18.05. Found: C, 61.89; H, 4.52; N, 18.03.

*4.1.6.4. 6-Benzyl-4-((2-chloro-4-nitrophenyl)imino)-3,4-dihydro-1,3,5-triazine-2(1H)-thione (**8d**).* Yellow powder, yield 98%, m.p. 70−72 °C. IR (KBr) ($\upsilon$, $cm^{-1}$): 3198 (NH), 3098, 3066 ($CH_{arom}$), 2923, 2850 ($CH_{aliph}$), 1625 (C═N), 1127 (C═S); $^1H$ NMR (DMSO-$d_6$) $\delta$: 3.60 (s, 2H, $CH_2$-ph), 6.66−7.74 (m, 8H, Ar-H, $J$ = 7.01 Hz), 8.73 (br. s, 1H, NH, $D_2O$ exchangeable), 9.09 (br. s, 1H, NH, $D_2O$ exchangeable); $^{13}C$ NMR (DMSO-$d_6$) $\delta$: 42.15, 112.28, 113.80, 114.78, 127.80, 128.90, 129.70, 135.04, 138.83, 147.60, 156.75, 169.95 ; MS (70 eV) $m/z$ (%): 374 ($M^+$, 19). Anal. calcd for $C_{16}H_{12}ClN5O_2S$ (373.82): C, 51.41; H, 3.24; N, 18.74. Found: C, 51.39; H, 3.21; N, 18.70.

**4.2. Biological Activity.** *4.2.1. In Vitro Cytotoxic Assay (MTT).* The potential cytotoxic properties of the prepared compounds **2−8** were evaluated against a panel of four human cancer cell lines, including hepatocellular carcinoma (HepG-2), prostate carcinoma (PC-3), breast adenocarcinoma (MCF-7), and non-small cell lung cancer cells (A-549), and the normal peripheral blood mononuclear cells (PBMCs) using the MTT assay[95] depending on the development of purple formazan crystals by mitochondrial dehydrogenases. More details were provided in Supporting Information.

*4.2.2. In Vitro Inhibition Assay of $EGFR^{WT}$ and Mutant $EGFR^{T790M}$ Activities.* The compounds that exhibited the most potent cytotoxic activity were further examined for their inhibitory activities against both $EGFR^{WT}$ and $EGFR^{T790M}$. A homogeneous time resolved fluorescence (HTRF) assay[96,97] was applied in this test with $EGFR^{WT}$ and $EGFR^{T790M}$ (Sigma). More details were provided in Supplementary Information.

*4.2.3. In Vivo Determination of p53 Ubiquitination.* The potential of different prepared derivatives as potent p53 ubiquitination inhibitors was evaluated using the standard procedure and protocol previously applied.[98,99] Briefly, cells were allowed to grow for 24 h to reach 50% confluency. Thereafter, of 1 $\mu$g p53, 4 $\mu$g MDM2 and 1 $\mu$g HIS-ubiquitin were transfected with the Gene Juice reagent, and then cells were grown for another 20 h. More details were provided in Supplementary Information.

**4.3. Molecular Modeling Study on $EGFR^{WT}$ and Mutant $EGFR^{T790M}$.** The domains of $EGFR^{WT}$ and mutant $EGFR^{T790M}$ kinase complexed with erlotinib and AZD9291 (PDB ID: 1M17 and 6JX0)[100,101] were downloaded from the Protein Data Bank. The docking calculations were done using MOE-Dock (Molecular Operating Environment) software version 2014.0901.[88,89] More details were provided in the Supplementary Information.

## ■ ASSOCIATED CONTENT

### Supporting Information

The Supporting Information is available free of charge at https://pubs.acs.org/doi/10.1021/acsomega.1c06836.

Experimental section; chemistry, *in vitro* cytotoxic assay (MTT), *in vitro* inhibition assay of $EGFR^{WT}$ and mutant $EGFR^{T790M}$ activities, *in vivo* determination of p53 ubiquitination, molecular modeling study on $EGFR^{WT}$ and mutant EGFRT790M, $^1H$-NMR spectra of the new compounds, $^{13}C$-NMR spectra of the new compounds, IR spectra of the new compounds, and mass spectra of the new compounds (PDF)

## ■ AUTHOR INFORMATION


### Corresponding Authors

**Manal M. Anwar** − *Department of Therapeutic Chemistry, National Research Centre, Cairo 12622, Egypt;* orcid.org/0000-0002-3967-4534; Email: manal.hasan52@live.com

**Abd El-Galil E. Amr** − *Pharmaceutical Chemistry Department, Drug Exploration & Development Chair (DEDC), College of Pharmacy, King Saud University, Riyadh 11451, Saudi Arabia; Applied Organic Chemistry Department, National Research Center, Cairo 12622, Egypt;* orcid.org/0000-0002-1338-706X; Email: aeamr1963@yahoo.com

### Authors

**Heba E. Hashem** − *Department of Chemistry, Faculty of Women, Ain Shams University, Cairo 11757, Egypt*

**Eman S. Nossier** − *Pharmaceutical Medicinal Chemistry and Drug Design Department, Faculty of Pharmacy (Girls), Al-Azhar University, Cairo 11754, Egypt*




https://doi.org/10.1021/acsomega.1c06836
ACS Omega 2022, 7, 7155−7171

**Eman M. Azmy** − *Department of Chemistry, Faculty of Women, Ain Shams University, Cairo 11757, Egypt*

Complete contact information is available at: https://pubs.acs.org/10.1021/acsomega.1c06836

### Notes

The authors declare no competing financial interest.

## ■ ACKNOWLEDGMENTS

The authors are grateful to the Deanship of Scientific Research, King Saud University, for funding through the Vice Deanship of Scientific Research Chairs.

## ■ REFERENCES

(1) Ewes, W. A.; Elmorsy, M. A.; El-Messery, S. M.; Nasr, M. N. A. Synthesis, biological evaluation and molecular modeling study of [1,2,4]-Triazolo[4,3-*c*] quinazolines: New class of EGFR-TK inhibitors. *Bioorg. Med. Chem.* **2020**, *28*, 115373.

(2) Shafei, A.; El-Bakly, W.; Sobhy, A.; Wagdy, O.; Reda, A.; Aboelenin, O.; Marzouk, A.; El Habak, K.; Mostafa, R.; Ali, M. A.; Ellithy, M. A review on the efficacy and toxicity of different doxorubicin nanoparticles for targeted therapy in metastatic breast cancer. *Biomed. Pharmacother.* **2017**, *95*, 1209−1218.

(3) Hassan, G. S.; Georgey, H. H.; Mohammed, E. Z.; George, R. F.; Mahmoud, W. R.; Omar, F. A. Mechanistic selectivity investigation and 2D-QSAR study of some new antiproliferative pyrazoles and pyrazolopyridines as potential CDK2 inhibitors. *Eur. J. Med. Chem.* **2021**, *218*, 113389.

(4) Lemmon, M. A.; Schlessinger, J. Cell signaling by receptor tyrosine kinases. *Cell* **2010**, *141*, 1117−1134.

(5) Kim, M.; Baek, M.; Kim, D. J. Protein Tyrosine signaling and its potential therapeutic implications in carcinogenesis. *Curr. Pharm. Des.* **2017**, *23*, 4226−4246.

(6) Bansal, R.; Malhotra, A. Therapeutic progression of quinazolines as targeted chemotherapeutic agents. *Eur. J. Med. Chem.* **2021**, *211*, 113016.

(7) Mokhtar, A. M.; El-Messery, S. M.; Ghaly, M. A.; Hassan, G. S. Targeting EGFR tyrosine kinase: Synthesis, *in vitro* antitumor evaluation, and molecular modeling studies of benzothiazole-based derivatives. *Bioorg. Chem.* **2020**, *104*, 104259.

(8) Zhang, H.; Berezov, A.; Wang, Q.; Zhang, G.; Drebin, J.; Murali, R.; Greene, M. I. ErbB receptors: from oncogenes to targeted cancer therapies. *J. Clin. Invest.* **2007**, *117*, 2051−2058.

(9) Othman, I. M. M.; Alamshany, Z. M.; Tashkandi, N. Y.; Gad-Elkareem, M. A. M.; Anwar, M. M.; Nossier, E. S. New pyrimidine and pyrazole-based compounds as potential EGFR inhibitors: synthesis, anticancer, antimicrobial evaluation and computational studies. *Bioorg. Chem.* **2021**, *114*, 105078.

(10) Ahmed, M. F.; Santali, E. Y.; El-Deen, E. M. M.; Naguib, I. A.; El-Haggar, R. Development of Pyridazine Derivatives as Potential EGFR inhibitors and Apoptosis Inducers: Design, Synthesis, Anticancer Evaluation, and Molecular Modeling Studies. *Bioorg. Chem.* **2021**, *106*, 104473.

(11) Capdevila, J.; Elez, E.; Macarulla, T.; Ramos, F. J.; Ruiz-Echarri, M.; Tabernero, J. Anti-epidermal growth factor receptor monoclonal antibodies in cancer treatment. *Cancer Treat. Rev.* **2009**, *35*, 354−363.

(12) Abd El-Meguid, E. A.; Moustafa, G. O.; Awad, H. M.; Zaki, E. R.; Nossier, E. S. Novel benzothiazole hybrids targeting EGFR: Design, synthesis, biological evaluation and molecular docking studies. *J. Mol. Struct.* **2021**, *1240*, 130595.

(13) Seshacharyulu, P.; Ponnusamy, M. P.; Haridas, D.; Jain, M.; Ganti, A. K.; Batra, S. K. Targeting the EGFR signaling pathway in cancer therapy. *Expert Opin. Ther. Targets* **2012**, *16*, 15−31.

(14) Kannaiyan, R.; Mahadevan, D. A comprehensive review of protein kinase inhibitors for cancer therapy. *Expert Rev. Anticancer Ther.* **2018**, *18*, 1249−1270.

(15) Petrelli, A.; Giordano, S. From single- to multi-target drugs in cancer therapy: When a specificity becomes an advantage. *Curr. Med. Chem.* **2008**, *15*, 422−432.

(16) Hawata, M. A.; El-Sayed, W. A.; Nossier, E. S.; Abdel-Rahman, A. A. H. Synthesis and Cytotoxic Activity of New Pyrimido [1, 2-c] quinazolines,[1, 2, 4] triazolo [4, 3-c] quinazolines and (quinazolin-4-yl)-1H-pyrazoles Hybrids. *Biointerface Res. Appl. Chem.* **2022**, *12*, 5217−5233.

(17) Xiao, Z.; Zhou, Z.; Chu, C.; Zhang, Q.; Zhou, L.; Yang, Z.; Li, X.; Yu, L.; Zheng, P.; Xu, S.; Zhu, W. Design, synthesis and antitumor activity of novel thiophene-pyrimidine derivatives as EGFR inhibitors overcoming T790M and L858R/T790M mutations. *Eur. J. Med. Chem.* **2020**, *203*, 112511.

(18) Barker, A. J.; Gibson, K. H.; Grundy, W.; Godfrey, A. A.; Barlow, J. J.; Healy, M. P.; Woodburn, J. R.; Ashton, S. E.; Curry, B. J.; Scarlett, L.; Henthorn, L.; Richards, L. Studies leading to the identification of ZD1839 (Iressa): an orally active, selective epidermal growth factor receptor tyrosine kinase inhibitor targeted to the treatment of cancer. *Bioorg. Med. Chem. Lett.* **2001**, *11*, 1911−1914.

(19) Khattab, R. R.; Alshamari, A. K.; Hassan, A. A.; Elganzory, H. H.; El-Sayed, W. A.; Awad, H. M.; Nossier, E. S.; Hassan, N. A. Click chemistry-based synthesis, cytotoxic activity and molecular docking of novel triazole-thienopyrimidine hybrid glycosides targeting EGFR. *J. Enzyme Inhib. Med. Chem.* **2021**, *36*, 504−516.

(20) Pao, W.; Miller, V. A.; Politi, K. A.; Riely, G. J.; Somwar, R.; Zakowski, M. F.; Kris, M. G.; Varmus, H. Acquired resistance of lung adenocarcinomas to gefitinib or erlotinib is associated with a second mutation in the EGFR kinase domain. *PLoS Med.* **2005**, *2*, 225−235.

(21) Ko, B.; Paucar, D.; Halmos, B. EGFR T790M: Revealing the secrets of a gatekeeper. *Lung Cancer* **2017**, *8*, 147−159.

(22) Yu, H. A.; Arcila, M. E.; Rekhtman, N.; Sima, C. S.; Zakowski, M. F.; Pao, W.; Kris, M. G.; Miller, V. A.; Ladanyi, M.; Riely, G. J. Analysis of tumor specimens at the time of acquired resistance to EGFR-TKI therapy in 155 patients with EGFR-mutant lung cancers. *Clin. Cancer Res.* **2013**, *19*, 2240−2247.

(23) El-Serwy, W. S.; Mohamed, N. A.; El-Serwy, W. S.; Nossier, E. S.; Mahmoud, K. Synthesis, molecular modeling studies and biological evaluation of novel pyrazole derivatives as antitumor and EGFR inhibitors. *Int. J. Pharm. Technol.* **2016**, *8*, 25192−25209.

(24) Xiao, Q.; Qu, R.; Gao, D.; Yan, Q.; Tong, L.; Zhang, W.; Ding, J.; Xie, H.; Li, Y. Discovery of 5-(methylthio) pyrimidine derivatives as L858R/T790M mutant selective Epidermal Growth Factor Receptor (EGFR) inhibitors. *Bioorg. Med. Chem.* **2016**, *24*, 2673−2680.

(25) Blair, J. A.; Rauh, D.; Kung, C.; Yun, C. H.; Fan, Q. W.; Rode, H.; Zhang, C.; Eck, M. J.; Weiss, W. A.; Shokat, K. M. Structure-guided development of affinity probes for tyrosine kinases using chemical genetics. *Nat. Chem. Biol.* **2007**, 229−238.

(26) Zhou, W.; Liu, X.; Tu, Z.; Zhang, L.; Ku, X.; Bai, F.; Zhao, Z.; Xu, Y.; Ding, K.; Li, H. Discovery of pteridin-7(8H)-one-based irreversible inhibitors targeting the epidermal growth factor receptor (EGFR) kinase T790M/L858R mutant. *J. Med. Chem.* **2013**, *56*, 7821−7837.

(27) Li, J.; An, B.; Song, X.; Zhang, Q.; Chen, C.; Wei, S.; Fan, R.; Li, X.; Zou, Y. Design, synthesis and biological evaluation of novel 2,4-diaryl pyrimidine derivatives as selective $EGFR^{L858R/T790M}$ inhibitors. *Eur. J. Med. Chem.* **2021**, *212*, 113019.

(28) Giaccone, G.; Wang, Y. Strategies for overcoming resistance to EGFR family tyrosine kinase inhibitors. *Cancer Treat. Rev.* **2011**, *37*, 456−464.

(29) Zhou, W.; Ercan, D.; Chen, L.; Yun, C. H.; Li, D.; Capelletti, M.; Cortot, A. B.; Chirieac, L.; Iacob, R. E.; Padera, R.; Engen, J. R.; Wong, K. K.; Eck, M. J.; Gray, N. S.; Jänne, P. A. Novel mutant-selective EGFR kinase inhibitors against EGFR T790M. *Nature* **2009**, *462*, 1070−1074.

(30) Ward, R. A.; Anderton, M. J.; Ashton, S.; Bethel, P. A.; Box, M.; Butterworth, S.; Colclough, N.; Chorley, C. G.; Chuaqui, C.; Cross, D. A. E.; Dakin, L. A.; Debreczeni, J. É.; Eberlein, C.; Finlay, M. R. V.; Hill, G. B.; Grist, M.; Klinowska, T. C. M.; Lane, C.; Martin, S.;

Orme, J. P.; Smith, P.; Wang, F.; Waring, M. J. Structure-and reactivity-based development of covalent inhibitors of the activating and gatekeeper mutant forms of the epidermal growth factor receptor (EGFR). *J. Med. Chem.* **2013**, *56*, 7025−7048.
(31) Kim, E. S. Olmutinib: first global approval. *Drugs* **2016**, *76*, 1153−1157.
(32) Song, J.; Jang, S.; Lee, J. W.; Jung, D.; Lee, S.; Min, K. H. Click chemistry for improvement in selectivity of quinazoline-based kinase inhibitors for mutant epidermal growth factor receptors. *Bioorg. Med. Chem. Lett.* **2019**, *29*, 477−480.
(33) Wang, Z.; Ye, W.; Qin, Y.; You, H.; Zhang, S.; Fan, F.; Wang, Y.; Zheng, L. Development and validation of a UPLC−MS/MS method for quantification of C-005, a novel third-generation EGFR TKI, and its major metabolite in plasma: Application to its first-in-patient study. *J. Chromatogr., B* **2021**, *1162*, 122475.
(34) Sequist, L. V.; Soria, J. C.; Goldman, J. W.; Wakelee, H. A.; Gadgeel, S. M.; Varga, A.; Papadimitrakopoulou, V.; Solomon, B. J.; Oxnard, G. R.; Dziadziuszko, R.; Aisner, D. L.; Doebele, R. C.; Galasso, C.; Garon, E. B.; Heist, R. S.; Logan, J.; Neal, J. W.; Mendenhall, M. A.; Nichols, S.; Piotrowska, Z.; Wozniak, A. J.; Raponi, M.; Karlovich, C. A.; Jaw-Tsai, S.; Isaacson, J.; Despain, D.; Matheny, S. L.; Rolfe, L.; Allen, A. R.; Camidge, D. R. Rociletinib in EGFR-mutated non−small-cell lung cancer. *N. Engl. J. Med.* **2015**, *372*, 1700−1709.
(35) Cross, D. A.; Ashton, S. E.; Ghiorghiu, S.; Eberlein, C.; Nebhan, C. A.; Spitzler, P. J.; Orme, J. P.; Finlay, M. R. V.; Ward, R. A.; Mellor, M. J.; Hughes, G.; Rahi, A.; Jacobs, V. N.; Brewer, M. R.; Ichihara, E.; Sun, J.; Jin, H.; Ballard, P.; al-Kadhimi, K.; Rowlinson, R.; Klinowska, T.; Richmond, G. H. P.; Cantarini, M.; Kim, D. W.; Ranson, M. R.; Pao, W. AZD9291, an irreversible EGFR TKI, overcomes T790M-mediated resistance to EGFR inhibitors in lung cancer. *Cancer Discovery* **2014**, *4*, 1046−1061.
(36) Cui, J. J. A New Challenging and Promising Era of Tyrosine Kinase Inhibitors. *ACS Med. Chem. Lett.* **2014**, *5*, 272−274.
(37) Zhou; Chen, G.; Gao, M.; Wu, J. Design, synthesis and evaluation of the osimertinib analogue (C-005) as potent EGFR inhibitor against NSCLC. *Bioorg. Med. Chem.* **2018**, *26*, 6135−6145.
(38) Jänne, P. A.; Yang, J. C. H.; Kim, D. W.; Planchard, D.; Ohe, Y.; Ramalingam, S. S.; Ahn, M. J.; Kim, S. W.; Su, W. C.; Horn, L.; Haggstrom, D.; Felip, E.; Kim, J. H.; Frewer, P.; Cantarini, M.; Brown, K. H.; Dickinson, P. A.; Ghiorghiu, S.; Ranson, M. AZD9291 in EGFR inhibitor-resistant non-small-cell lung cancer. *N. Engl. J. Med.* **2015**, *372*, 1689−1699.
(39) Moreno, L. M.; Quiroga, J.; Abonia, R.; Lauria, A.; Martorana, A.; Insuasty, H.; Insuasty, B. Synthesis, biological evaluation, and *in silico* studies of novel chalcone- and pyrazoline-based 1,3,5-triazines as potential anticancer agents. *RSC Adv.* **2020**, *10*, 34114.
(40) Martins, P.; Jesus, J.; Santos, S.; Raposo, L. R.; Roma-Rodrigues, C.; Baptista, P. V.; Fernandes, A. R. Heterocyclic Anticancer Compounds: Recent Advances and the Paradigm Shift towards the Use of Nanomedicine's Tool Box. *Molecules* **2015**, *20*, 16852−16891.
(41) Facchetti, G.; Rimoldi, I. Anticancer platinum (II) complexes bearing *N*-heterocycle rings. *Bioorg. Med. Chem. Lett.* **2019**, *29*, 1257−1263.
(42) Roskoski, R., Jr. Properties of FDA-approved small molecule protein kinase inhibitors. *Pharmacol. Res.* **2019**, *144*, 19−50.
(43) Liu, H.-B.; Gao, W.-W.; Tangadanchu, V. K. R.; Zhou, C.-H.; Geng, R.-X. Novel aminopyrimidinyl benzimidazoles as potentially antimicrobial agents: Design, synthesis and biological evaluation. *Eur. J. Med. Chem.* **2018**, *143*, 66−84.
(44) Alp, M.; Göker, H.; Brun, R.; Yıldız, S. Synthesis and antiparasitic and antifungal evaluation of 2′-arylsubstituted-1H,1′H-[2,5′]bisbenzimidazolyl-5-carboxamidines. *Eur. J. Med. Chem.* **2009**, *44*, 2002−2008.
(45) Hu, Z.; Ou, L.; Li, S.; Yang, L. Synthesis and biological evaluation of 1-cyano-2-amino benzimidazole derivatives as a novel class of antitumor agents. *Med. Chem. Res.* **2014**, *23*, 3029−3038.
(46) Akhtar, M. J.; Siddiqui, A. A.; Khan, A. A.; Ali, Z.; Dewangan, R. P.; Pasha, S.; Yar, M. S. Design, synthesis, docking and QSAR study of substituted benzimidazole linked oxadiazole as cytotoxic agents, EGFR and erbB2 receptor inhibitors. *Eur. J. Med. Chem.* **2017**, *126*, 853−869.
(47) Demirel, S.; Kilcigil, G. A.; Kara, Z.; Güven, B.; Beşikci, A. O. Synthesis and Pharmacologic Evaluation of Some Benzimidazole Acetohydrazide Derivatives as EGFR Inhibitors. *Turk. J. Pharm. Sci.* **2017**, 285−289.
(48) Cheong, J. E.; Zaffagni, M.; Chung, I.; Xu, Y.; Wang, Y.; Jernigan, F. E.; Zetter, B. R.; Sun, L. Synthesis and anticancer activity of novel water soluble benzimidazole carbamates. *Eur. J. Med. Chem.* **2018**, *144*, 372−385.
(49) Ayhan-Kilcigil, G.; Kuş, C.; Çoban, T.; Özdamar, E. D.; Can-Eke, B. Identification of a Novel Series of *N* -Phenyl-5-[(2-phenylbenzimidazol-1-yl)methyl]-1,3,4-oxadiazol-2-amines as Potent Antioxidants and Radical Scavengers. *Arch. Pharm.* **2014**, *347*, 276−282.
(50) Celik, İ.; Ayhan-Kılcıgil, G.; Guven, B.; Kara, Z.; Gurkan-Alp, A. S.; Karayel, A.; Onay-Besikci, A. Design, synthesis and docking studies of benzimidazole derivatives as potential EGFR inhibitors. *Eur. J. Med. Chem.* **2019**, *173*, 240−249.
(51) Kaur, P.; Chawla, A. 1,2,4-triazole: a review of pharmacological activities. *Int. Res. J. Pharm.* **2017**, *8*, 10−29.
(52) Rose, C.; Vtoraya, O.; Pluzanska, A.; Davidson, N.; Gershanovich, M.; Thomas, R.; Johnson, S.; Caicedo, J. J.; Gervasio, H.; Manikhas, G.; Ayed, F. B.; Burdette-Radoux, S.; Chaudri-Ross, H. A.; Lang, R. An open randomized trial of second-line endocrine therapy in advanced breast cancer: comparison of the aromatase inhibitors letrozole and anastrozole. *Eur. J. Cancer* **2003**, *39*, 2318−2327.
(53) Dahmani, R.; Manachou, M.; Belaidi, S.; Chtita, S.; Boughdiri, S. Structural characterization and QSAR modeling of 1,2,4-triazole derivatives as α-glucosidase inhibitors. *New J. Chem.* **2021**, *45*, 1253−1261.
(54) Lønning, P.; Pfister, C.; Martoni, A.; Zamagni, C. Pharmacokinetics of third-generation aromatase inhibitors. *Semin. Oncol.* **2003**, *30*, 23−32.
(55) Lønning, P. E.; Geisler, J.; Dowsett, M. Pharmacological and clinical profile of anastrozole. *Breast Cancer Res. Treat.* **1998**, *49*, S53−S57.
(56) Njar, V. C. O.; Brodie, A. M. H. Comprehensive pharmacology and clinical efficacy of aromatase inhibitors. *Drugs* **1999**, *58*, 233−255.
(57) Goss, P. E. Pre-clinical and clinical review of vorozole, a new third generation aromatase inhibitor. *Cancer Res. Treat.* **1998**, *49*, S59−S65.
(58) El-Faham, A.; Farooq, M.; Almarhoon, Z.; Abd Alhameed, R.; Wadaan, M. A. M.; de la Torre, B. G.; Albericio, F. Di-and tri-substituted s-triazine derivatives: Synthesis, characterization, anti-cancer activity in human breast-cancer cell lines, and developmental toxicity in zebrafish embryos. *Bioorg. Chem.* **2020**, *94*, 103397.
(59) Cascioferro, S.; Parrino, B.; Spanò, V.; Carbone, A.; Montalbano, A.; Barraja, P.; Diana, P.; Cirrincione, G. 1,3,5-Triazines: A promising scaffold for anticancer drugs development. *Eur. J. Med. Chem.* **2017**, *142*, 523−549.
(60) Nie, Z.; Perretta, C.; Erickson, P.; Margosiak, S.; Lu, J.; Averill, A.; Almassy, R.; Chu, S. Structure-based design and synthesis of novel macrocyclic pyrazolo[1,5-a] [1,3,5] triazine compounds as potent inhibitors of protein kinase CK2 and their anticancer activities. *Bioorg. Med. Chem. Lett.* **2008**, *18*, 619−623.
(61) Zhang, B.; Zhang, Q.; Xiao, Z.; Sun, X.; Yang, Z.; Gu, Q.; Liu, Z.; Xie, T.; Jin, Q.; Zheng, P.; Xu, S.; Zhu, W. Design, synthesis and biological evaluation of substituted 2-(thiophen-2-yl)-1,3,5-triazine derivatives as potential dual PI3Kα/mTOR inhibitors. *Bioorg. Chem.* **2020**, *95*, 103525.
(62) Lolak, N.; Akocak, S.; Bua, S.; Sanku, R. K. K.; Supuran, C. T. Discovery of new ureido benzenesulfonamides incorporating 1,3,5-


https://doi.org/10.1021/acsomega.1c06836
*ACS Omega* 2022, 7, 7155−7171

triazine moieties as carbonic anhydrase I, II, IX and XII inhibitors. *Bioorg. Med. Chem.* **2019**, *27*, 1588−1594.
(63) Havránková, E.; Csöllei, J.; Vullo, D.; Garaj, V.; Pazdera, P.; Supuran, C. T. Novel sulfonamide incorporating piperazine, amino-alcohol and 1,3,5-triazine structural motifs with carbonic anhydrase I, II and IX inhibitory action. *Bioorg. Chem.* **2018**, *77*, 25−37.
(64) Żołnowska, B.; Sławiński, J.; Szafrański, K.; Angeli, A.; Supuran, C. T.; Kawiak, A.; Wieczór, M.; Zielińska, J.; Bączek, T.; Bartoszewska, S. Novel 2-(2-arylmethylthio-4-chloro-5-methylbenzenesulfonyl)-1-(1,3,5-triazin-2-ylamino) guanidine derivatives: Inhibition of human carbonic anhydrase cytosolic isozymes I and II and the transmembrane tumor-associated isozymes IX and XII, anticancer activity, and molecular modeling studies. *Eur. J. Med. Chem.* **2018**, *143*, 1931−1941.
(65) Hashem, H. E.; Amr, A. E.-G. E.; Nossier, E. S.; Elsayed, E. A.; Azmy, E. M. Synthesis, antimicrobial activity and molecular docking of novel thiourea derivatives tagged with thiadiazole, imidazole and triazine moieties as potential DNA gyrase and topoisomerase IV inhibitors. *Molecules* **2020**, *25*, 2766.
(66) Zhou, X.; Lin, K.; Ma, X.; Chui, W. K.; Zhou, W. Design, synthesis, docking studies and biological evaluation of novel dihydro-1,3,5-triazines as human DHFR inhibitors. *Eur. J. Med. Chem.* **2017**, *125*, 1279−1288.
(67) Narva, S.; Chitti, S.; Amaroju, S.; Bhattacharjee, D.; Rao, B. B.; Jain, N.; Alvala, M.; Sekhar, K. V. G. C. Design and synthesis of 4-morpholino-6-(1,2,3,6-tetrahydropyridin-4-yl)-N-(3,4,5-trimethoxyphenyl)-1,3,5-triazin-2-amine analogues as tubulin polymerization inhibitors. *Bioorg. Med. Chem. Lett.* **2017**, *27*, 3794−3801.
(68) Wong, J. R.; Morton, L. M.; Tucker, M. A.; Abramson, D. H.; Seddon, J. M.; Sampson, J. N.; Kleinerman, R. A. Risk of subsequent malignant neoplasms in long-term hereditary retinoblastoma survivors after chemotherapy and radiotherapy. *Am. J. Clin. Oncol.* **2014**, *32*, 3284.
(69) Dehnhardt, C. M.; Venkatesan, A. M.; Chen, Z.; Delos-Santos, E.; Ayral-Kaloustian, S.; Brooijmans, N.; Yu, K.; Hollander, I.; Feldberg, L.; Lucas, J.; Mallon, R. Identification of 2-oxatriazines as highly potent pan-PI3K/mTOR dual inhibitors. *Bioorg. Med. Chem. Lett.* **2011**, *21*, 4773−4778.
(70) Koh, M.; Lee, J. C.; Min, C.; Moon, A. A novel metformin derivative, HL010183, inhibits proliferation and invasion of triple-negative breast cancer cells. *Bioorg. Med. Chem.* **2013**, *21*, 2305−2313.
(71) Kim, E. S. Enasidenib: first global approval. *Drugs.* **2017**, *77*, 1705−1711.
(72) Keldsen, N.; Havsteen, H.; Vergote, I.; Bertelsen, K.; Jakobsen, A. Altretamine (hexamethylmelamine) in the treatment of platinum-resistant ovarian cancer: a phase II study. *Gynecol. Oncol.* **2003**, *88*, 118−122.
(73) Guo, H.; Diao, Q. P. 1, 3, 5-Triazine-azole Hybrids and their Anticancer Activity. Curr. Top. *Med. Chem.* **2020**, *20*, 1481−1492.
(74) Daştan, A.; Kulkarni, A.; Török, B. Environmentally benign synthesis of heterocyclic compounds by combined microwave-assisted heterogeneous catalytic approaches. *Green Chem.* **2012**, *14*, 17−37.
(75) Kaur, N.; Kishore, D. Microwave-Assisted Synthesis of Six-Membered *O*-Heterocycles. *Synth. Commun.* **2014**, *44*, 3047−3081.
(76) Kaur, N. Microwave-Assisted Synthesis of Five-Membered *O*-Heterocycles. *Synth. Commun.* **2014**, *44*, 3483−3508.
(77) Diaz-Ortiz, A.; Moreno, A.; Sanchez-Migallon, A.; Prieto, P.; Carrillo, J. R.; Vazquez, E.; Gomez, M.; Herrero, M. A. Microwave-assisted reactions in heterocyclic compounds with applications in medicinal and supramolecular chemistry. *Comb. Chem. High Throughput Screening* **2007**, *10*, 877−902.
(78) De la Hoz, A.; Loupy, A. Eds. *Microwaves in Organic Synthesis*; 3rd ed.; Wiley-VCH: Weinheim, Germany, 2012, 127−207.
(79) Amr, A. E.-G. E.; Mageid, R. E. A.; El-Naggar, M.; Naglah, A. M.; Nossier, E. S.; Elsayed, E. A. Chiral Pyridine-3, 5-bis-(L-phenylalaninyl-L-leucinyl) Schiff Base Peptides as Potential Anticancer Agents: Design, Synthesis, and Molecular Docking Studies Targeting Lactate Dehydrogenase-A. *Molecules* **2020**, *25*, 1096.
(80) Abd El-Meguid, E. A.; El-Deen, E. M. M.; Nael, M. A.; Anwar, M. M. Novel benzimidazole derivatives as anti-cervical cancer agents of potential multi-targeting kinase inhibitory activity. *Arab. J. Chem.* **2020**, *13*, 9179−9195.
(81) Srour, A. M.; Ahmed, N. S.; Abd El-Karim, S. S.; Anwar, M. M.; El-Hallouty, S. M. Design, synthesis, biological evaluation, QSAR analysis and molecular modelling of new thiazol-benzimidazoles as EGFR inhibitors. *Bioorg. Med. Chem.* **2020**, *28*, 115657.
(82) Othman, I. M. M.; Gad-Elkareem, M. A. M.; Amr, A. E.-G. E.; Al-Omar, M. A.; Nossier, E. S.; Elsayed, E. A. Novel heterocyclic hybrids of pyrazole targeting dihydrofolate reductase: design, biological evaluation and in silico studies. *J. Enzyme Inhib. Med. Chem.* **2020**, *35*, 1491−1502.
(83) Dawood, D. H.; Nossier, E. S.; Ali, M. M.; Mahmoud, A. E. Synthesis and molecular docking study of new pyrazole derivatives as potent anti-breast cancer agents targeting VEGFR-2 kinase. *Bioorg. Chem.* **2020**, *101*, 103916.
(84) Anwar, M. M.; Abd El-Karim, S. S.; Mahmoud, A. H.; Amr, A. E.-G. E.; Al-Omar, M. A. A Comparative Study of the Anticancer Activity and PARP-1 Inhibiting Effect of Benzofuran−Pyrazole Scaffold and Its Nano-Sized Particles in Human Breast Cancer Cells. *Molecules* **2019**, *24*, 2413.
(85) Zhang, J.; Yang, P. L.; Gray, N. S. Targeting cancer with small molecule kinase inhibitors. *Nat. Rev. Cancer.* **2009**, *9*, 28−39.
(86) Khattab, R. R.; Hassan, A. A.; Osman, D. A. A.; Abdel-Megeid, F. M.; Awad, H. M.; Nossier, E. S.; El-Sayed, W. A. Synthesis, anticancer activity and molecular docking of new triazolo [4, 5-d] pyrimidines based thienopyrimidine system and their derived N-glycosides and thioglycosides. *Nucleos Nucleot Nucl.* **2021**, *40*, 1090−1113.
(87) Mowafy, S.; Galanis, A.; Doctor, Z. M.; Paranal, R. M.; Lasheen, D. S.; Farag, N. A.; Jänne, P. A.; Abouzid, K. A. M. Toward discovery of mutant EGFR inhibitors; Design, synthesis and *in vitro* biological evaluation of potent 4-arylamino-6-ureido and thioureido-quinazoline derivatives. *Bioorg. Med. Chem.* **2016**, *24*, 3501−3512.
(88) Zhao, Z.; Wu, H.; Wang, L.; Liu, Y.; Knapp, S.; Liu, Q.; Gray, N. S. Exploration of type II binding mode: a privileged approach for kinase inhibitor focused drug discovery ? *ACS Chem. Biol.* **2014**, *9*, 1230−1241.
(89) Furet, P.; Caravatti, G.; Lydon, N.; Priestle, J. P.; Sowadski, J. M.; Trinks, U.; Traxler, P. Modelling study of protein kinase inhibitors: binding mode of staurosporine and origin of the selectivity of CGP 52411. *J. Comput.-Aided Mol. Des.* **1995**, *9*, 465−472.
(90) Liu, Y.; Gray, N. S. Rational design of inhibitors that bind to inactive kinase conformations. *Nat. Chem. Biol.* **2006**, *2*, 358−364.
(91) Abou Elmagd, W. S. I.; Hemdan, M. M.; Samy, S. S.; Youssef, A. S. A. Thiosemicarbazide Derivatives as Building Block in Synthesis of Target Heterocyclic Compounds with Their Antimicrobial Assessment. *J. Heterocycl. Chem.* **2017**, *54*, 1391−1395.
(92) Hemdan, M. M.; El-Sayed, A. A. E. Use of Phthalimidoacetyl Isothiocyanate as a Scaffold in the Synthesis of Target Heterocyclic Systems, and Their Antimicrobial Assessment. *Chem. Pharm. Bull.* **2016**, *64*, 483−489.
(93) El-Sayed, A. A.; Atta-allah, S. R.; Hemdan, M. M. Utility of 3- ( thiophen-2-yl ) prop-2-enoyl isothiocyanate in heterocyclic synthesis. *J. Chem. Res.* **2019**, *43*, 1−8.
(94) Hemdan, M. M.; Abou Elmagd, W. S.; Samy, S. S.; Youssef, A. S. Dodecanoyl thiosemicarbazide derivatives as useful synthons in the synthesis of 1, 2, 4-triazole, 1, 3, 4-thiadiazole, and 1, 3-benzothiazole derivatives. *Synth. Commun.* **2016**, *46*, 710−718.
(95) Nossier, E. S.; El-Hallouty, S. M.; Zaki, E. R. Synthesis, anticancer evaluation and molecular modeling of some substituted thiazolidinonyl and thiazolyl pyrazole derivatives. *Int. J. Pharm. Pharm. Sci.* **2015**, *7*, 353−359.
(96) Kassem, A. F.; Moustafa, G. O.; Nossier, E. S.; Khalaf, H. S.; Mounier, M. M.; Al-Yousef, S. A.; Mahmoud, S. Y. *In-vitro* anticancer potentiality and molecular modelling study of novel amino acid derivatives based on $N^1$, $N^3$-bis-(1-hydrazinyl-1-oxopropan-2-yl) isophthalamide. *J. Enzyme Inhib. Med. Chem.* **2019**, *34*, 1247−1258.


https://doi.org/10.1021/acsomega.1c06836
*ACS Omega* 2022, 7, 7155−7171

(97) Jia, Y.; Quinn, C. M.; Gagnon, A. I.; Talanian, R. Homogeneous time-resolved fluorescence and its applications for kinase assays in drug discovery. *Anal. Biochem.* **2006**, *356*, 273−281.
(98) El-Sayed, A. A.; Nossier, E. S.; Almehizia, A. A.; Amr, A. E.-G. E. Design, synthesis, anticancer evaluation and molecular docking study of novel 2, 4-dichlorophenoxymethyl-based derivatives linked to nitrogenous heterocyclic ring systems as potential CDK-2 inhibitors. *J. Mol. Struct.* **2022**, *1247*, 131285.
(99) Amr, A. E.-G. E.; Elsayed, E. A.; Al-Omar, M. A.; Badr Eldin, H. O.; Nossier, E. S.; Abdallah, M. M. Design, synthesis, anticancer evaluation and molecular modeling of novel estrogen derivatives. *Molecules* **2019**, *24*, 416.
(100) Nossier, E. S.; Abd El-Karim, S. S.; Khalifa, N. M.; El-Sayed, A. S.; Hassan, E. S. I.; El-Hallouty, S. M. Kinase inhibitory activities and molecular docking of a novel series of anticancer pyrazole derivatives. *Molecules* **2018**, *23*, 3074.
(101) Yan, X. E.; Ayaz, P.; Zhu, S. J.; Zhao, P.; Liang, L.; Zhang, C. H.; Wu, Y. C.; Li, J. L.; Choi, H. G.; Huang, X.; Shan, Y.; Shaw, D. E.; Yun, C. H. Structural basis of AZD9291 selectivity for EGFR T790M. *J. Med. Chem.* **2020**, *63*, 8502−8511.
(102) Mohi El-Deen, E. M.; Abd El-Meguid, E. A.; Hasabelnaby, S.; Karam, E. A.; Nossier, E. S. Synthesis, docking studies, and *in vitro* evaluation of some novel thienopyridines and fused thienopyridine−quinolines as antibacterial agents and DNA gyrase inhibitors. *Molecules* **2019**, *24*, 3650.
(103) Abd El-Karim, S. S.; Mohamed, H. S.; Abdelhameed, M. F.; Amr, A. E.-G. E.; Almehizia, A. A.; Nossier, E. S. Design, synthesis and molecular docking of new pyrazole-thiazolidinones as potent anti-inflammatory and analgesic agents with TNF-$\alpha$ inhibitory activity. *Bioorg. Chem.* **2021**, *111*, 104827.



https://doi.org/10.1021/acsomega.1c06836
*ACS Omega* 2022, 7, 7155−7171